# TOWER CONTAMINATION AND RADIATION TEMPORAL VARIABILITY IN A DOUGLAS FIR FOREST

[SHUAI HAO]
[March, 2016]

SUPERVISORS:
[Dr. Ir. C. van der Tol]
[Prof. Dr. Z. Su]

# TOWER CONTAMINATION AND RADIATION TEMPORAL VARIABILITY IN A DOUGLAS FIR FOREST

SHUAI HAO
Enschede, The Netherlands, [March, 2016]

Thesis submitted to the Faculty of Geo-Information Science and Earth Observation of the University of Twente in partial fulfilment of the requirements for the degree of Master of Science in Geo-information Science and Earth Observation.
Specialization: [Water Resource]

SUPERVISORS:
[Dr. Ir. C. van der Tol]
[Prof. Dr. Z. Su]

THESIS ASSESSMENT BOARD:
[Dr. Ir. S. Salama (Chair)]
[Dr. Chen Shi (Associate Professor
College of Resource Environment and Tourism
Capital Normal University)]

ABSTRACT

Solar radiation is a key factor trigger the land-atmosphere reaction. The albedo as the ratio of reflected to incoming shortwave radiation is very crucial factor influences the energy storage of the land surface. To explore the variability of the radiation and albedo in forest, a 46 meters height measurement tower, standing in the central of Netherlands, provides us a valuable opportunity of radiation determination in the ouglas fir forest (needle-leaved forest). But an ignorable matter is that the tower-based measurement would unavoidably be influenced by the tower itself. With the two types of net radiometers (cnr1 and cnr4) installed different height of the measurement tower, we are able to quantifying the tower contamination effects and explore the diurnal variability of the radiation in the forest.

as a result, with 10 meters distance in vertical, shortwave radiation and net radiation diurnal variability in the clear skies normally symmetry in the local sun noon and irregularly fluctuation in cloudy skies; for longwave radiation, the values keep irregular fluctuation in all sky condition. The difference between the two instruments results shows: for incoming shortwave radiation, the cnr1 result could higher than CNR4 result up to 10% and for outgoing shortwave radiation, the CNR1 result is much lower, the difference is up to 40%;The result of longwave is quite matched; the difference of net radiation measurements is relatively larger. With the same surroundings and homogeneous radiative condition during the study period, we speculated that the tower contamination is referable with the solar zenith angle. The result shows the highest difference existed while the solar zenith angle is minimum.

Meanwhile, the albedo temporal variability shows a 'U' shape cycle while the smallest value exists in the noon and the highest value occurs in the morning and afternoon. Also the forest reflected more radiation back to space in winter than the summer time: the albedo in the summer clear skies in around 0.7 to 0.9 in the day time and from 0.12 to 0.16 in the winter. Also we investigated the relationship between the albedo and solar zenith angle: we can conclude no matter in the summer or winter, albedo decreased with solar zenith angle decreased.The study managed to help us to understand the radiation and albedo temporal variability in the needle-leaved forest. Further more, provides others researchers an reliable result on quantify the tower-based radiaiton measurement.

**Key words**: diurnal solar radiation; albedo; temporal variability; solar zenith angle; tower-based measurement; net radiometers; needle-leaved forest;

# ACKNOWLEDGEMENTS

I would like to express my grateful to all of the people who supported me during the study life in ITC. Frist of all, I would like to give my honest gratitude to my first supervisor Dr. Ir. C. van der Tol and my second supervisor Prof. Dr. Z. Su for their patient and generous support on my thesis. During the whole thesis period, they have shown a great sense of responsibility and talented wisdom, keep giving me valuable opinion. This thesis wouldn't been finished without their support.
I would like to thank all the staff in ITC; especially in water resource department for their unforgettable help during my study in ITC: dr.ir. S. Salama; ir. A.M. van Lieshout; dr.ir. C.M.M. Mannaerts; ir. G.N. Parodi;dr; dr. Y. Zeng;M.W. Lubczynski; dr.ing. T.H.M. Rientjes;dr.ir. W.J. Timmermans dr. Z. Vekerdy ; dr.ir. R. van der Velde;L. Wang, M. Ucer;ete……
I also very grateful to PHD candidate C.R. Cisneros Vaca and X.Yuan and all of the kindly students whom have shared their insightful understanding on my thesis.
Thanks to my family and all my friends here.

# Table of Contents

# LIST OF FIGURES

# LIST OF TABLES

# 1. BACKGOUND

## 1.1. Introduction

To understand the spatial and temporal dynamics of the diurnal surface radiation budget components of forests is inextricably linked to water resources management which plays an important role in the land–atmosphere interactions. Land surface albedo, as the reflection coefficient (or ∝), acts as a great contribution to the planetary radiative energy budget (Bastable et al. 1993) . The albedo significantly influences the energy storage of the land surface (Khan et al. 2015; Singh et al. 2014). And it is impactful to the atmosphere near the land surface and the available energy for the heating the ground (Wizemann et al. 2014). The energy absorbed at the surface is partly used to drive vegetation processes such as evapotranspiration, photosynthesis and carbon assimilation and the remaining fraction controls evaporation, snow melt and temperature related processes at the soil surface (Pinty et al., 2008). All these processes will consequently decide the available energy partitioned to the flux of the ground, latent and sensible heat at the top of the vegetation canopy. The albedo is treated as the crucial fundamental factor to characterize the surface energy budget of lower atmosphere, and it has an indispensability meaning to the different land surface conditions operating at various temporal scales (Weligepolage, Gieske, & Su, 2013). Previous studies investigated the temporal variabilities of albedo in the Tibetian Plateau (Wang et al. 2004; Zhong and Yinhai 1988; Tian, Zhang, and Zhu 2014), frozen soil (Wu et al. 2015) and snow area (Ghatak, Sinsky, and Miller 2014; Lee et al. 2016). Besides, the albedo of forests has attracted more attention by scientists and public (Peng et al. 2015; Houldcroft et al. 2009).The miscalculation of albedo could lead the errors in the estimation of surface temperature, heat and energy calculation in land-atmosphere interactions. In recently years, many researchers have investigated to the study of the relationship between the solar zenith angle and albedo, obtained valuable experience. (Monteith and Szeicz 1961) indicated what while the solar zenith angle varies from $20°$ to $60°$, the albedo decreased from 0.19 to 0.16. . (Liu, Wang, and Fu 2008), (Guan et al. 2009)and (Roxy, Sumithranand, and Renuka 2010) study shown the diurnal albedo variability appeared 'U' shape and have an exponential relationship with solar zenith angle. Thus the negligence of solar zenith angle would consequently leads the mis-estimation of albedo variability exploration.

Nowadays, the radiation, albedo and some other physical characteristic of the Earth could be obtained by the in-situ measurement, as well as satellite remote sensing techniques. Normally, the in-situ measurement is widely used to acquire the different kind of energy parameters' datasets, because of the limitation of the precise degree of the satellite. However, there exist some inevitable problem along with the in-situ measurement. The high datasets accuracy and reliability have been required for more and more scientific studies. As for measuring the radiations in the forest, the uncertainty of the instruments and difference of radiation measurement which was caused by the tower contamination is a very interested point. Some previous researchers have noticed that based on the measurement tower, the influence from the measurement tower affected the data in different extents (Amiro and Sheppard 1994; Wilson and Meyers 2007).

The pyrometers only supposed to measure the reflected radiation (Gardner and Jones 1980), but during the measuring, it also captures the tower reflected (Liang et al. 2017) and the near-horizon light from the sky (Manara et al. 2016). Eventually, those two inference factors will lead the inaccurateness in the radiation and albedo estimation. In order to eliminate the tower contamination, a mask have been designed by (Ide et al. 2016). The contamination effects on diurnal variations of spectral reflectance, the relationship between masking and open condition and vegetation indices are been calculated, respectively. As a conclusion, they summarized in the clear sky, the specular reflection from the tower is attributed to its position. Also the structure and tower's colour could also attributed to the contamination effects. Meanwhile, the assessment and quantification of the measurements errors are the crucial and necessary step before the data collection and difference quantifying. In previous studies, the statistics estimator r-squared (Pedersen et al. 2016; Noi, Kappas, and Degener 2016; Ladner et al. 2014) and root-mean-squared-error (RMSE)(Román et al. 2013; Shantikumar et al. 2016; Gavilán 2016; Shi et al. 2014) have been widely adopted to check the discrepancy and accuracy for testing the difference between the net radiometers .

In this study tower-based solar radiation measurements data will be used, which had been installed for providing the precise in-situ measurement and reliable observation datasets in the centre of Netherlands. The primality measurement focuses on a small region of study area (roughly 1 $km^2$), the CNR1 and CNR4 net radiometers, the four-component radiometer (Gavilan, Berengena, and Allen 2007; Blonquist, Tanner, and Bugbee 2009), installed on the top of measurement tower with will be applied to determine the albedo over time series.

The CNR1 net radiometer was installed at 35 meters height of the tower, CNR4 at 46 m height. The tower itself will reflect the radiation from the sky and surroundings. However, there are a few questions during the measurement. One of the main contaminations is caused by the tower. When a wide-angle downward-facing spectrometer is used for tower-based measurements of reflected radiation, it also captures reflections from the tower and near-horizon light from the sky within the field of view, leading to incorrect canopy reflectance estimates (Ide et al. 2016). Thus, tower contamination has to be taken into consideration before studying the variability of albedo in the study area. The agreement between the instruments is a very important issue for analysis the subsequent data, in particularly of radiation measurement is the fundamental step before or during larger experiments.

In short, this study mainly focuses on the tower contamination to the measurement results and the temporal variability of the radiations. Moreover, the influence of the solar zenith angle has been investigated as well. The purpose of study was achieved by the instruments certainty tests, the radiation results collection in the central of Netherlands and the variable calculation and its analysis.

The structure of paper is as follows. Some of the ideal theoretical description such as solar radiation budget, diurnal radiation are briefly given. The specifically description of study area, the experiment for instruments consistency test, tower measurement and the result assessment procedure is presented. Finally the conclusion are given in the last part.

## 1.2. Surface radiation budget

The Earth's surface radiation budget is deemed particularly pointing the fluxes through a plane at Earth-atmosphere interface. Two mainly objects is included in radiation budget, one the solar radiation flux (shortwave) and the other is terrestrial radiation flux (longwave).

### 1.2.1. Incoming shortwave

Emission of solar radiation, the incoming shortwave, during the transmission will be interfered by the backscattered by substance in the air, the cloud absorption and reflection, absorbed by water vapor dust and reflected by the surface , the last is been absorbed by the land.

$$R_{ns} = R_{sin} - R_{sout} = (1 - \alpha)R_{sin}$$

Where $R_{ns}$ is the total solar radiation, $R_{sin}$ represents the incoming radiation, $R_{sout}$ is the reflected solar radiation (outgoing shortwave) and $\alpha$ is albedo (MacWhorter and Weller 1991).

### 1.2.2. Longwave

Terrestrial radiation flux, referred as the longwave radiation, is emitted by the sky and air. The outgoing longwave transmission is basically approaching the net emission by water vapor, emission by clouds, absorbed by clouds water vapor.

Longwave radiation is calculated by the Stefan-Boltzmann equation (Wang et al. 2005):

$$L_{IN} = \varepsilon\sigma T_a^4$$

Where $\varepsilon$ is the emissivity, $\sigma$ is $5.670373\times10^{-8}$ W $m^{-2}$ $K^{-4}$ as the Stefan-Boltzmann constant, $T_a$ is the surface temperature in Kelvin.

## 1.3. Objective

The objectives of this study are:

- To quantify the consistency between radiation measurements carried out at two different heights in a Douglas fir forest
- To explore the temporal variability of radiation and tower contamination
- To explore the relationship between the solar zenith angle and tower contamination
- To explore temporal variability of albedo
- To quantify the relationship between the solar zenith angle and albedo

# 2. METHODOLOGY

## 2.1. Study area

The Speulderbos (Figure 1), a forest near the village Garderen ( $52^{\circ}05'08.1"N,\ 5^{\circ}41'25.8"E$ ) is part of a large forested area in the central part in the Netherlands. The Douglas fir is the dominant species in the observation area. The area is mostly flat terrain and elevation may reach 110m above sea level in some areas. In 2016, the average height of the trees was observed to be around 33 m.

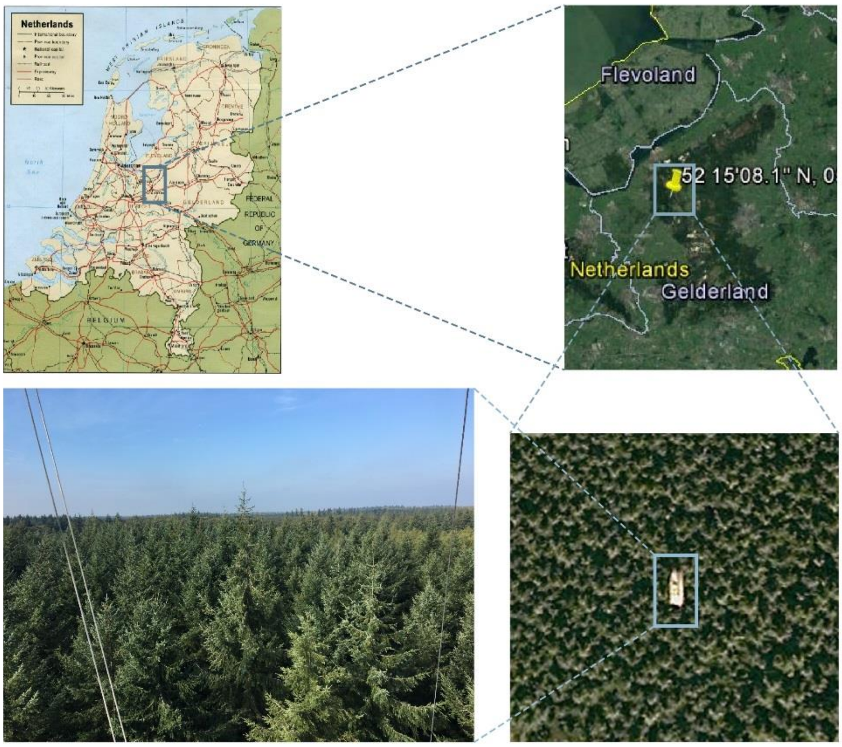


Figure 2.1 location and surroundings of study area

## 2.2. Meteorological conditions

The main targets of the study is to quantify tower contamination effects and the temporal variability of radiations and albedo, the scatter and diffuse would leads the discrepancy on radiation measurement , in this case the identification of clear and cloudy skies should be proceed.

Data of meteorological conditions were downloaded from the Royal Netherlands Meteorological Institute (KNMI) database, which provides the cloud cover and visibility, temperature, wind and precipitation information in days, as a method of sky identification.

Meanwhile the skies classification can also been done by the diurnal cycles of irradiance. Since the KNMI data provides the hourly cloud cover index, we can analysis the diurnal radiation performance by checking the hourly meteorological data.

```
"# STN,YYYYMMDD,   HH,   DD,   FH,   FF,   FX,    T,  T10,   TD,   SQ,    Q,   DR,   RH,     P,   VV,    N,    U,   WW,   IX,    M,    R,    S,
O,    Y"

"  260,20110101,    1,  240,   30,   30,   40,   36,     ,   34,    0,    0,    0,   -1,10217,    5,    7,   99,   32,    7,    1,    1,    0,
0,    0"
"  260,20110101,    2,  250,   30,   20,   50,   36,     ,   35,    0,    0,    0,    0,10214,    2,    1,   99,   34,    7,    1,    0,    0,
0,    0"
"  260,20110101,    3,  260,   30,   30,   50,   39,     ,   38,    0,    0,    0,   -1,10211,    4,    4,   99,   32,    7,    1,    1,    0,
0,    0"
"  260,20110101,    4,  270,   30,   30,   50,   42,     ,   37,    0,    0,    0,   -1,10208,   21,    8,   97,   51,    7,    1,    1,    0,
0,    0"
"  260,20110101,    5,  260,   30,   30,   50,   42,     ,   38,    0,    0,    0,   -1,10204,   39,    8,   97,   23,    7,    0,    1,    0,
0,    0"
```

Figure 2.2 example of KNMI meteorology data

The STN is the code of the KNMI station. In hour study, the station "De Bilt" located close to the measurement tower, thus the data from "De Bilt" have been used here. "HH" represents the time of the day in hour. "N" column represents the cloud cover information, which 9 means the invisible sky and means the sky is totally clear.

### 2.3. Method

In order to determine the diurnal solar variability, two types of net radiometers, CNR1 and CNR4 (Kipp and Zonen, The Netherlands.) were used to measure the solar radiation, the incoming radiation coming from sky and the one faces downward is used to measure the reflected solar radiation. Utilizing the data from above instruments, albedo, the ratio of reflected, incoming radiation and outgoing radiation, can be determined.

The study of diurnal solar variability was achieved by the detection and calibration of incoming (Rsin) and reflected (Rsout) solar radiation, the incoming (Rsin) and reflected (Rsout) longwave radiation, albedo (α) and the solar zenith angle (SZA).

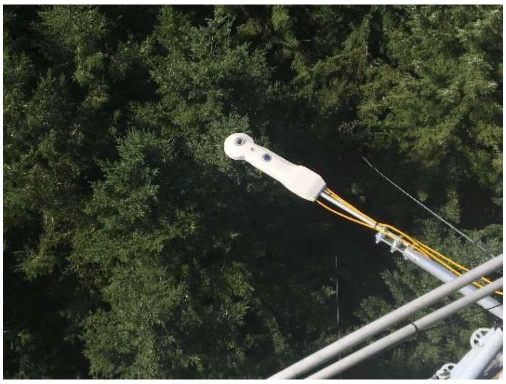

Figure 2.3 Net radiometer

A CNR1 net radiometer have been install on a measurement tower in study area at 35 meters height which provides us the solar radiation data over one year. At the same time, the incident solar radiation and emitted radiation from sky and air were reaching tower body, effects the sensor detected result. Thus, the reliability of the CNR1 data is been questioned. Another net radiometer, a CNR4, has been used for quantifying the contamination from the tower. However, for two different type of net radiometers, it is necessary to figure out if the two instruments have a good consistency or not.

An experiment has been designed for quantifying the consistency between the two net radiometers in a same condition at the same time.

### 2.3.1. Instruments intercomparison

The intercomparison between two instruments have been processed in ITC garden, on the 16th May (Figure 3). The two instruments were installed behind to each other at the same height which is 1.5 meters.

To ensure the data reliability, exclude the possible shadow cover on the instruments, the study period of all types of radiation are been set from 10 a.m. to 14 p.m. The study area covered with the homogeneity of surroundings.

CNR1 and CNR4 net radiometers were connected to the same CR23X data logger which has used for collection of instantaneous radiation measurements and the data stored as 1 min averages.

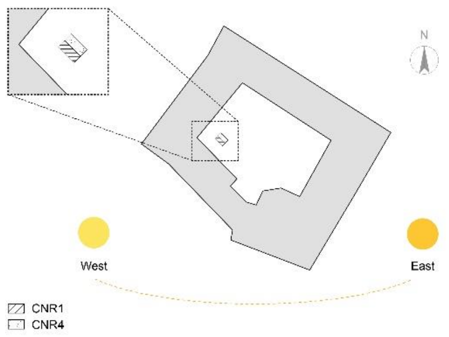


Figure 2.4 Intercomparison experiment in ITC garden. The "gray" shaded area represents the building, the open area the garden.

The net radiometers designed as a combination of 2 pyranometers (CM for determining the incoming and reflected solar radiation (0.3-3µm) and 2 pyrgeometers (CG3) for determining the incoming and outgoing far infrared radiation (5-50µm).

The results show the value of all types of radiations were detected by the instruments.

As the intercomparison for the instruments has been finished, the CNR4 has been installed on the top of the tower for helping quantify the tower contamination.

A widely used statistics estimators Root-mean-square error (RMSE) and correlation coefficient R (Chai and Draxler 2014) are been used in determination of the data discrepancy and reliability.

RMSE is a measurement of differences between values:

$$\mathrm{RMSE} = [\frac{1}{n}\sum_{t=1}^{n}(P_i - Q_i)^2]^{0.5}$$

R is calculated by:

$$\mathrm{R} = \sum_{i=1}^{n}(P_i - \overline{P})(Q_i - \overline{Q})/[\sum_{t=1}^{n}(P_i - \overline{P})^2\sum_{i=1}^{n}(Q_i - \overline{Q})^2]^{0.5}$$

Where the n is the number of data pairs, Pi is the values measured by CNR1 and $Q_i$ is the measured value of CNR4. $\overline{P}$ is the mean value of CNR 1 and $\overline{Q}$ is the mean value of CNR 4.Meanwhile the regression slopes were also considered. R is used to test the consistency of two instruments. RMSE is to measurement discrepancy.

In this case, Matlab (matrix laboratory) is been used to processed the following data and calculation the discrepancy.

Table 2.1 Specifications of the pyranometers of the radiometers CNR1 and CNR4 used in this study

| Specification | Type of net radiometers | |
|---|---|---|
| | CNR1 | CNR4 |
| Specification | Type of net radiometers | |
| | CNR1 | CNR4 |
| Spectral range | 305 ~ 3000 nm short-wave<br>4.4 ~ 50 μm long-wave | 300 ~ 2800 nm short-wave<br>4.5 ~ 42 μm long-wave |
| Sensitivity | 10 ~ 35 μV/W/m² shortwave<br>5 ~ 10 μV/W/m² longwave | 7 ~ 20 μV/W/m² shortwave<br>5 ~ 10 μV/W/m² longwave |
| Response time | <18 s | < 18 s |
| Non-linearity (over full range) | <2.5 % | < 1 % |
| Temperature dependence of sensitivity (-10 °C to +40 °C) | <4% | < 5 % |
| Field of view | 180 ° shortwave sensor<br>150 ° longwave sensor | 180 ° shortwave sensor<br>150 ° longwave sensor |
| Operating temperature | -40 °C to +80 °C | -40 °C to +80 °C |

### 2.3.2. Tower measurement

The measurement tower about 3 meter length and 2 meter width, iron made scaffold of 46 m height, standing in the center of the study area, surrounding by the Douglas fir. CNR1 and CNR4 have been set in the measurement tower in 35 and 45 meters respectively. The two upward sensors of CNR1 and CNR4 receive the incoming radiation and incoming longwave radiation from space, also the CNR1 received the reflected solar radiation by the tower body; two downwards sensor detecting the outgoing shortwave and longwave from the downwelling direction, the reflected outgoing radiation would be captured by sensors as well. The data be recorded in 1 minute interval.

Figure 2.5 picture of measurement tower in study area

Both of net radiometers pointing to the south, 2 meters away from the measurement tower in order to avoid the shadow cover over the instruments.

Figure 2.6 shows the side view of measurement tower. CNR1 which have been installed near the canopy would receive the reflected radiation in all kinds of radiation. CNR4 was installed on top of the tower in September in 2016, the view of upward sensor rarely received reflected solar radiation from the tower. The downward sensor received upwelling outgoing radiation, inevitably received the reflected radiation from the tower as well.

The independent radiation measurement of CNR1 period was from 27th February in 2015 to 27th February in 2016.And the coverage of measurement period of CNR1 and CNR4 was from 16th till 31th October in 2016.

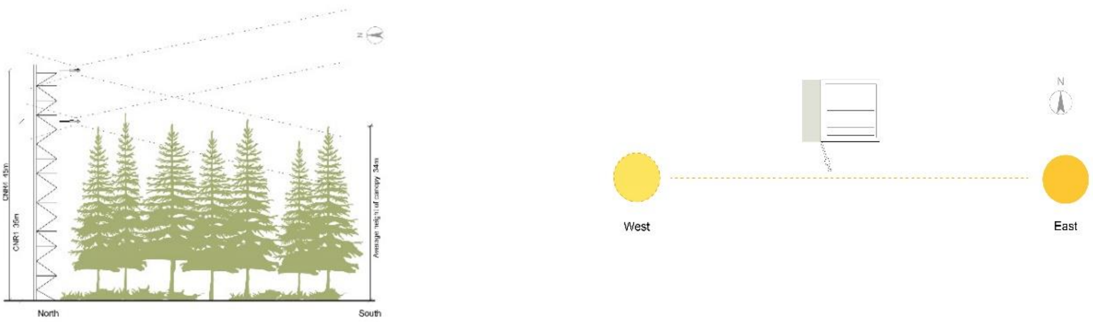


Figure 2.6 schematic diagram of tower measurement (a) side view of the tower, instruments and surrounding trees (b) top-view of the tower measurement

### 2.4. Variables calculation

- Net radiation

In the ordinary situation, the value of net radiation at surface is due to the difference of incoming and outgoing shortwave plus longwave radiation fluxes. The net shortwave flux (Shaw 1956) depends on the incident solar radiation the albedo α. The net longwave flux are rely on the downwelling longwave radiation and the surface emissivity ($\varepsilon$) and temperature($T$).

$$Rn = Rs_{in} - Rs_{out} + Rl_{in} - Rl_{out}$$

Where the $Rl_{in}$ (W/m²) indicates the incoming longwave (measured by the downward-facing sensor of both two net radiometers), $Rl_{out}$ (W/m²) indicates the outgoing longwave (measured by the upward-facing sensor of both two net radiometers).

- Albedo

Albedo was calculated as the ratio of reflected to incoming shortwave radiation (Betts and Ball 1997):

$$\alpha = Rs_{out} / Rs_{in}$$

In order to guarantee the reliability of the data set, reduce the uncertainty resulted by unstable and heterogeneous radiative conditions, the albedo calculation focused on times when the incoming shortwave is greater than 10 W/m².

- Solar zenith angle

The solar zenith angle (SZA) is the angle between the zenith and the centre of the sun's disc and the solar zenith angle is related to the Julian DOY, longitude and latitude (Shupe and Intrieri 2004). An ideally sketch description has been given in Figure 6, on the 21th March and September the solar zenith angle supposed be 0 degree in the mid of the day.

In our study, the measurement site located in the central of Netherlands, a high latitudes area. The solar zenith angle changes with the Julian DOY, and does not reach 0 degrees in any situation.

Matlab was used for processing the data. All those data was been recorded by the instruments and the output data from radiometer all been proceed into ascii text format. The data where are obviously beyond the range of physical possibility were rejected.

For quantifying the relationship between albedo and solar zenith angle, the unreliable data due to the directional response in low solar elevation have been removed. Based on the KNMI data, the typically clear day which have significantly characteristic and cloudy skies have been identified.

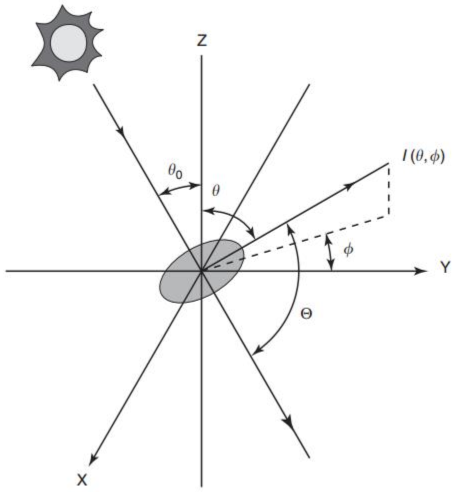


Figure 2.7
Orientation of incident sunlight and reflected light. $\theta_o$ indicates the solar zenith angle, $\theta$ is represent the view zenith angle, $\phi$the relativeazimuth angle, and $\Theta$ t he scattering angle. The incident sunlight is taken to be in the YZ plane

# 3. RESULTS AND DISCUSSION

## 3.1. Intercomparison between CNR1 and CNR4

The weather was characterized by clear sky during the intercalibration of the two instruments on 17th May 2015. Figure 7 shows that, the results indicates about a highly consistency of the two net radiometers in radiation measurements. During the study period when they were installed in the same target in the ITC garden, the maximum incoming shortwave is greater than 500 $Wm^{-2}$; the maximum outgoing shortwave is around 83 $Wm^{-2}$; and the incoming longwave range is from 320 to 375 $Wm^{-2}$, the outgoing longwave is between 387 and 410 $Wm^{-2}$ during the whole experiment period. Meanwhile, the net radiation was among 0 and 450 $Wm^{-2}$ during the selected time period. The slopes of linear regression in this experiment were around 1:1.

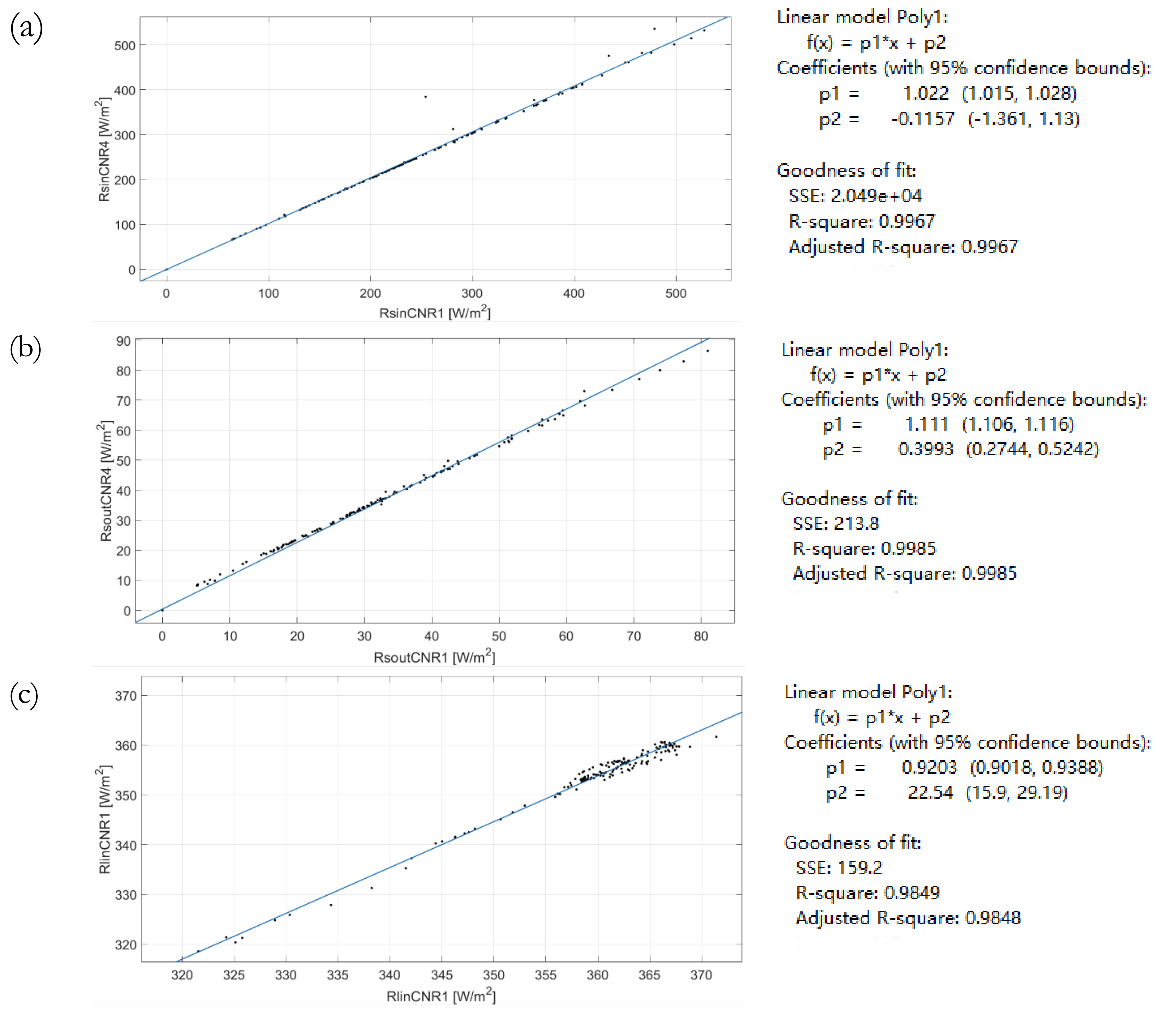

(d)

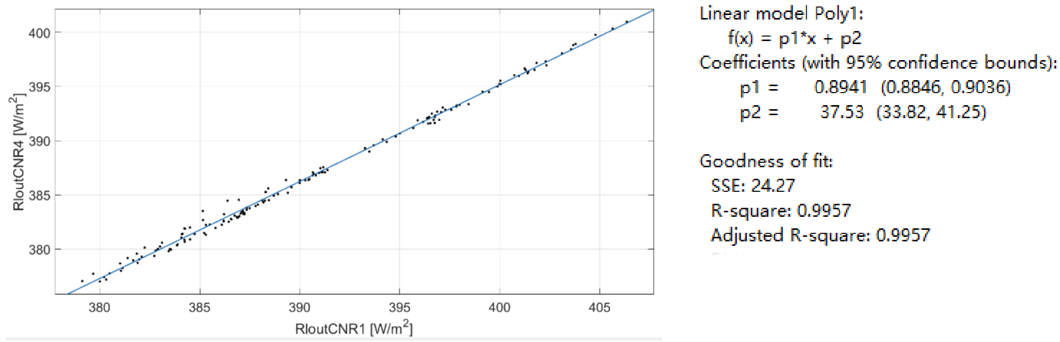


(e)

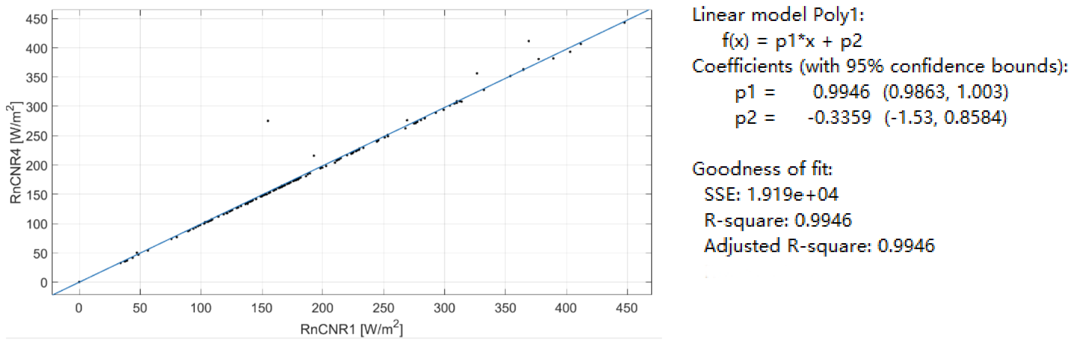


Figure 3.1 Scatterplot of intercomparison with radiationbetween CNR1 and CNR4 and details (14 to 17May 2016): (a) incoming shortwave radiation (b) outgoing shortwave radiation (c) incoming longwave radiation (d) outgoing longwave radiation (e) net radiation.

For the radiometers comparison, the difference between the two instruments were plotted in Figure 3.2. The statistics assessment results have been presented in Table 3.1.

Table 3.1 Statistics of the CNR1 and CNR4 comparison

| | Rsin | Rsout | Rlin | Rlout | Rn |
|---|---|---|---|---|---|
| R | 0.9983 | 0.9992 | 0.9924 | 0.9978 | 0.9972 |
| RMSE | 8.2 | 19.7 | 6.5 | 5.3 | 12.6 |
| Averaged value($Wm^{-2}$) | 444.8 | 32.9 | 334.7 | 383.6 | 331.8 |
| Original difference($Wm^{-2}$) | 14.0 | 6.1 | 8.0 | 3.9 | 5.1 |
| Weight | 3% | 16.8% | 2% | 1% | 1.5% |

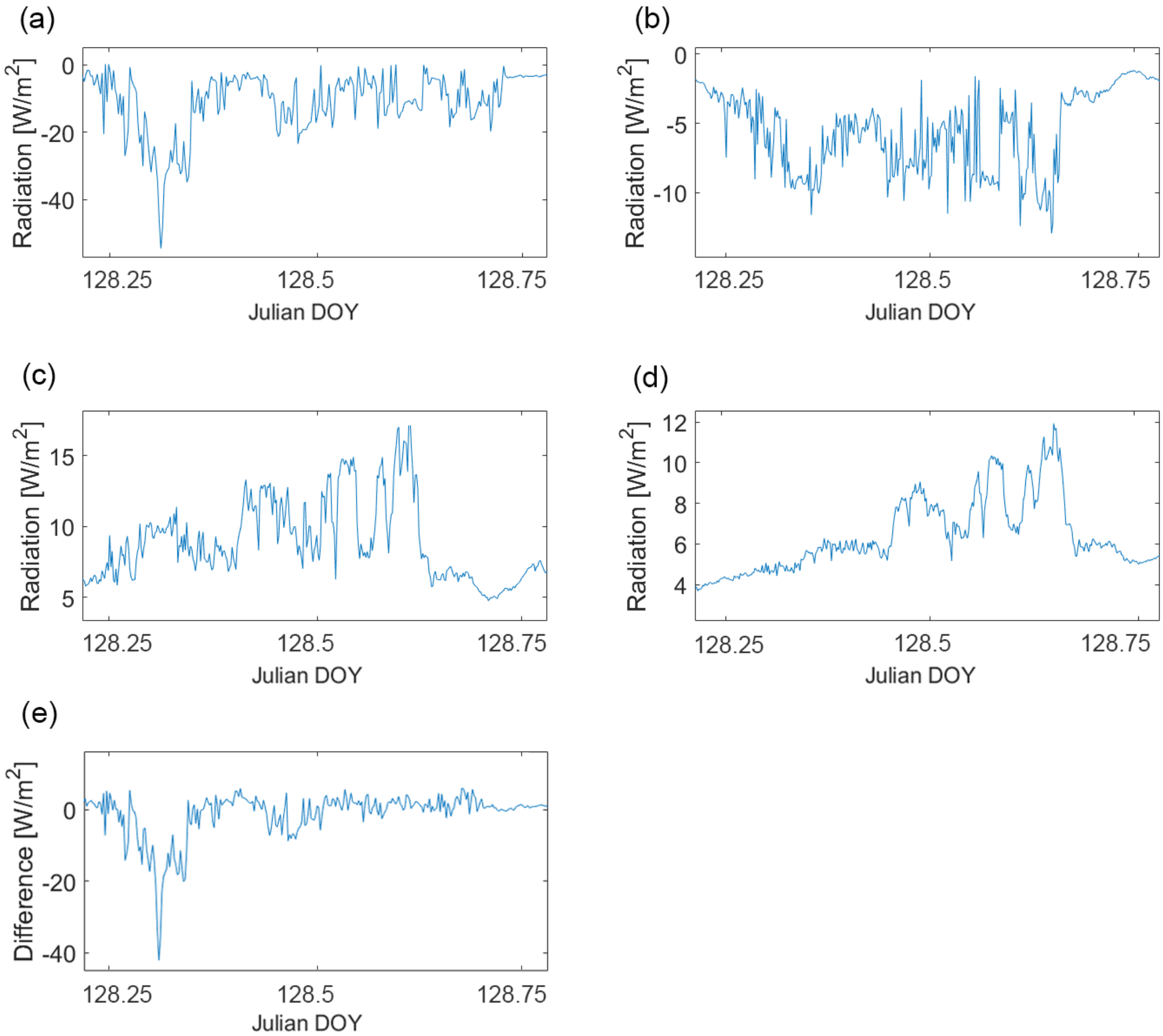


Figure 3.2 Difference between CNR1 and CNR4 radiation measurement result (a) the incoming shortwave radiation (b) the outgoing shortwave radiation (c) the incoming longwave radiation (d) the outgoing longwave radiation (e) the net radiation (all in $Wm^{-2}$)

**Assessment of shortwave radiation**

The result shows the range of the difference from two instrument are approximately round 2 to 60 $Wm^{-2}$ for incoming shortwave and 1 to 14 $Wm^{-2}$ for outgoing shortwaves.

The maximum incoming difference between two instruments was 58 $Wm^{-2}$, while the radiation value is 477 and 419 Wm-2 for each of the instruments. The instant increase of difference happened round 10a.m. For the rest of the day, the amplitude of difference remains within 20 Wm-2 and the average difference was 14 Wm-2. The original difference between the incoming shortwave was about 3% in incoming shortwave between the two instruments. The relatively high difference exists in the comparison of outgoing shortwave which up to 16.8%. We speculated the difference was due to the un-homogeneous surroundings, the sensors detected the reflectance from the brushwood, buildings in different direction and different distance. As a recommendation, the difference of outgoing shortwave would be determined more precise and reliable if the experiment been proceeded in a homogeneous environment with the same underlay.

The reason may due to a transient shadow covered of one the instrument that made the detected incoming radiation value suddenly got lower.

The difference of outgoing shortwave is much less. The difference max value of outgoing shortwave is 14 $Wm^{-2}$ while the outgoing shortwave is 68 and 83 $Wm^{-2}$.

Table 3.1 shows for incoming and outgoing shortwave, the RMSE was quite small. The R is very high for both of incoming and outgoing shortwave (greater than 0.99) depicts the two instruments are quite consistent with each other.

**Assessment of longwave radiation**

Figure 3.2 (c) (d) shows the difference of incoming and outgoing longwave radiation. For incoming longwave, the differences were approximately from 5 to 18 Wm-2, while the average was 8.0 Wm-2 for incoming longwave and 3.9 $Wm^{-2}$ outgoing longwave. There are no significant amplitude or huge difference between the two instruments. The original difference was about 2% during the day time.

Well consistency was been observed during the longwave intercomparison, R of both instruments were greater than 0.98.

**Assessment of net radiation**

The intercomparison shown in Figure 3.2(e).The statistics shows the differences range for net radiation between 0 to 40 Wm-2 (CNR1 & CNR4), the average value of difference between is round 5.1 Wm-2. There is no remarkable increase or decrease in the difference between the two radiometers during the study period. The net radiation accuracy checking in an important steps for multi instruments measurement. The original difference of net radiation was about 1.5% between two instruments during the day.

However, the peak of the differences appeared in the 10 a.m. which may cause by the difference of incoming radiation at that time. The difference of RMSE value is 1.8 $Wm^{-2}$ while the range of net radiation is up to 450 $Wm^{-2}$. R was greater than 0.99. It's indicates the instruments have a very good consistency.

As a summary, the comparison results between the CNR1 and CNR4 shows those two instruments agree well to each other. Meanwhile we should notice the temporal stability of the experiment should be done in a longer period. Due to the geography conditions limitation in Netherlands, very few clear skies occurred in the May, and the dataset was not adequate for studying the temporal stability.

## 3.2. Temporal variability of radiaions and tower contamination

The well consistency have been proved in section 3.1, based on the well agreement between CNR1 and CNR4, we begin to explore the effect factors on the measurement radiation results. As the CNR1 and CNR4 closed to the tower body and kept receiving the reflected radiations, the tower contamination is considered as the main influence factor contribute to the difference between solar radiations.

During the study period, the recognition of clear and cloudy skies are treated as the basic step of quantifying the tower contamination. In an ideal clear skies, the solar radiation directly reach the net radiation without been scattered by molecules or suspensoids in the atmosphere. But ideal clear sky is not always encountered. Thus, the definition of clear sky should base on the principle that the cloud cover index have to as small as possible. The 16$^{th}$ October 2016 (DOY 290 in 2016), 23$^{th}$ October 2016 (DOY

297 in 2016) and 21th October 2016 (DOY 295 in 2016) have been selected as the clear and cloudy skies. Table 3.2 shows from the 6:00 a.m. till 6:00 p.m. the cloudy cover situation of each hour of the days.

Table 3.2 Cloud cover index

| Hour of day | Cloud cover index | | |
|---|---|---|---|
| | 10/16/2016 | 10/23/2016 | 10/21/2016 |
| 6:00 | 2 | 0 | 9 |
| 7:00 | 5 | 0 | 9 |
| 8:00 | 6 | 0 | 9 |
| 9:00 | 0 | 3 | 9 |
| 10:00 | 0 | 0 | 8 |
| 11:00 | 6 | 0 | 7 |
| 12:00 | 4 | 0 | 3 |
| 13:00 | 4 | 0 | 2 |
| 14:00 | 0 | 0 | 8 |
| 15:00 | 0 | 0 | 8 |
| 16:00 | 0 | 0 | 8 |
| 17:00 | 0 | 4 | 8 |
| 18:00 | 4 | 3 | 8 |

During the day time in 16th October, the sky had a slightly cloud cover at noon for two hours; on 23th, the day can be treated as a typical clear sky because rarely cloud cover appeared. On the 21th, the sky was almost been covered by cloudy for whole day, identified as a cloud day. The data observed under clear sky is more meaningful study of radiation variation and difference study, while overcast condition sky is under unstable and heterogeneous radiative conditions.

### 3.2.1. Temporal variability and tower contamination of shortwave radiation

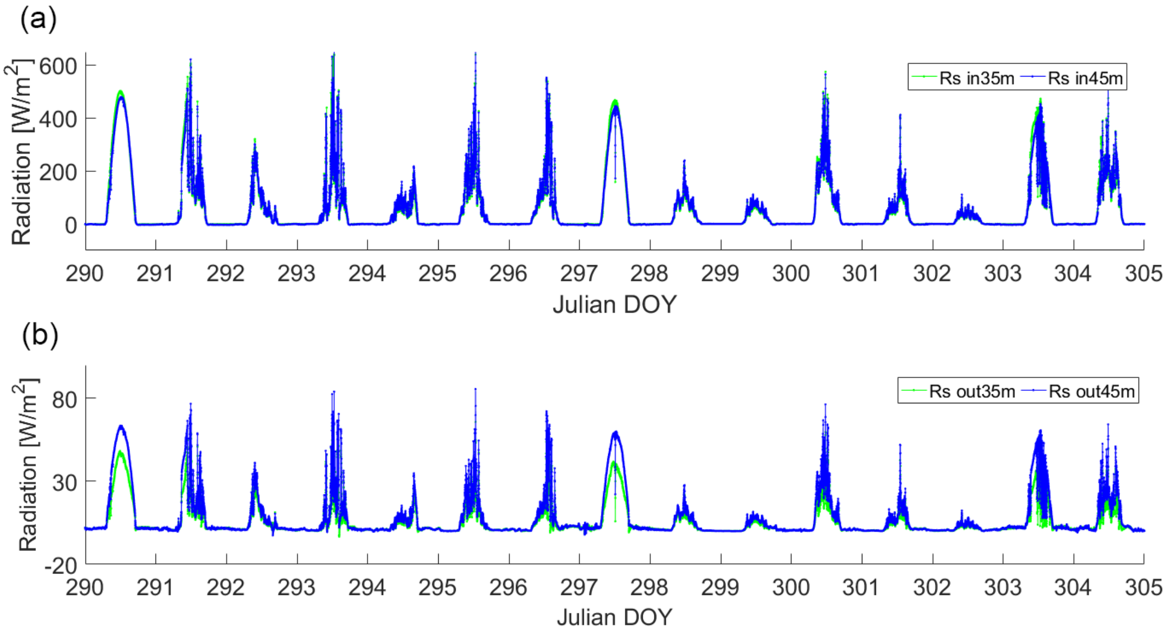


Figure 3.3 diurnal changes of incoming and outgoing shortwave radiation. (a) incoming shortwave variation (b) outgoing shortwave variation

Figure 3.4 shows the diurnal variation of shortwave radiation over the study period. The near-surface diurnal shortwave variability are mainly influenced by the solar position during the day.
The shortwave curves in clear skies have the same characteristic and tendency. During the diurnal radiation cycles, the curve is smooth and they are symmetric around noon. The highest values occurred in the mid of the day.
The overcast sky have a difference performance. After the beginning of rise up of, the curves of shortwave started oscillate intensely. For each of the cloudy skies, the highest measured values is no longer the only occurrence during the noon of the day time, as in clear skies. The peak of the shortwave for both incoming and outgoing occurred in different period of time during the cloudy skies situation.
For example, based on the data from CNR4, the highest value in DOY 291 is 620 $Wm^{-2}$ for incoming radiation 77 $Wm^{-2}$ for outgoing, in 11:00; but in DOY 296, the peak occurs in 12:30, 550 $Wm^{-2}$ for incoming and 73 $Wm^{-2}$ for outgoing shortwave radiation. The amplitude of radiation value is much higher than those which under clear skies situation, the tendency were irregular and disorganized.

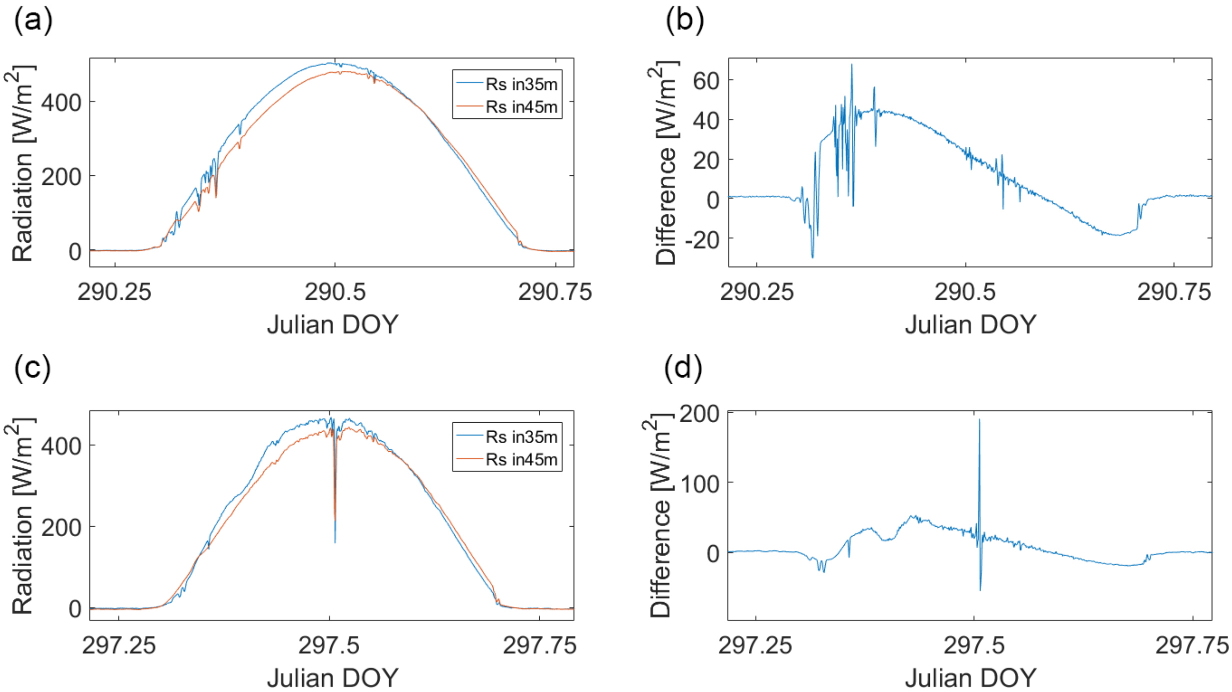


Figure 3.4 comparison and differences of incoming shortwave radiation in clear-skies (a) comparison of incoming shortwave radiation DOY 290 (b) differences of incoming shortwave radiation in DOY 290 (c) comparison of incoming shortwave radiation DOY 297 (d) differences of incoming shortwave radiation in DOY 297

Table 3.3 incoming shortwave radiation average difference and peak information of clear skies

| Time(Julian DOY) | Peak time(Julian DOY) | | Peak value ($Wm^{-2}$) | | Average difference of daytime ($Wm^{-2}$) |
|---|---|---|---|---|---|
| | CNR1 | CNR4 | CNR1 | CNR4 | |
| 290 (clear) | 290.5 | 290.5 | 502 | 479 | 15.1 |
| 297 (clear) | 297.6 | 297.6 | 468 | 442 | 9.6 |

The diurnal variation of incoming radiation of DOY 290 and 297 is shown in Figure 3.5. The incoming radiation increased round 8:00 in the morning (DOY 290.25) and the peak happened at noon (DOY 290.5). However, in the Figure 3.5(c), DOY 297, the value of radiation have a sudden-drop down in the noon, last about 1 minute. The drop is most likely caused by a cloudy shadow covering. During the elevation procedure before noon, value from CNR1 is always larger than CNR4. Some of the slightly amplitude are caused by the cloud covering.

A dramatic performance happened in both of the two days after the noon. The measured value start getting close. Around 13:00, the difference between the two instruments equal to 0 $Wm^{-2}$. Than the CNR4 measured data is a little bit larger than the CNR1 till the end of daytime.

To definite the possible affect factor, firstly the tree shadow was considered to be responsible for this phenomenon. After the field reconnaissance it was been cleared that none of the height of the tree was higher 35 meters, it is means no shadow covering on the CNR1. Thus the phenomenon are treated caused by the tower body. Referred to Figure 2.7(a), the CNR1 have been set in 35 meters, which is 10m lower than the CNR4. The upward-facing sensor on CNR4 was set in the top of the tower, the figure indicates that the sensor was no longer influenced by the tower reflectance, all the sources of incoming radiation is directly from the sun illumination. But the situation is different for CNR1. The sensor on CNR1 was not only received the radiation from the sun illumination, but also received the reflectance radiation by the tower, which causes the main difference.

The result shown the tower reflected from the east side was higher than west side in the morning and lower in the afternoon. The CNR1 installed at 35 meters height was a little bit closed to the right side of the measurement tower Figure 2.7(b). In the morning, sun rises with increasingly incoming solar radiation. The reflected radiation from the tower started to appear. When the sun moved from the east to west, the reflected radiation received by the sensor getting lower at the same time because the reflected area on the tower front side were decreased.

The largest difference in DOY 290 is 75 $Wm^{-2}$ occurred in the early morning. During that time, the sky was covered by clouds for few hours Under the unstable radiative condition, the diffusion and backscattered of shortwave happened caused sensor of both instruments detected irregular and abnormal noisy in clear skies situation.

The largest difference in DOY 297 is almost up to 200 $Wm^{-2}$ occurred in the middle of the day. At the same moment the incoming radiation have a huge amplitude in a seconds. After that difference came to -30 $Wm^{-2}$.

.

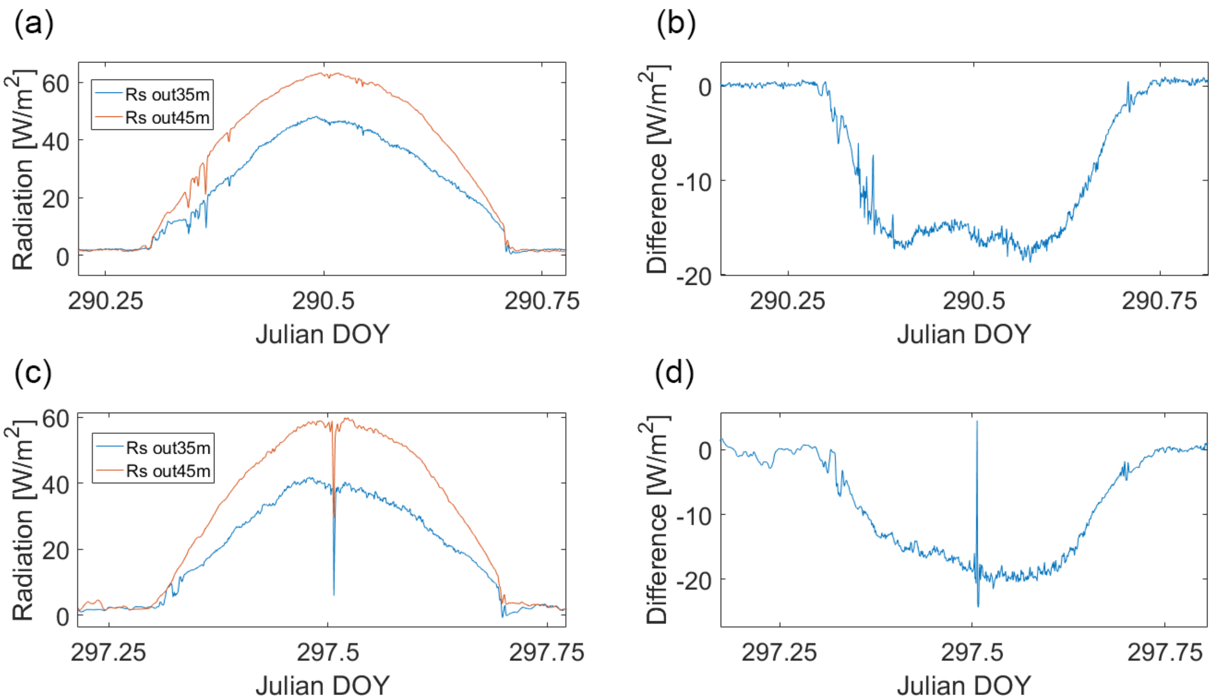


Figure 3.5 comparison and differences of outgoing shortwave radiation in clear-skies (a) comparison of outgoing shortwave radiation DOY 290 (b) differences of outgoing shortwave radiation in DOY 290 (c) comparison of outgoing shortwave radiation DOY 297 (d) differences of outgoing shortwave radiation in DOY 297

The Figure 3.6 shows the outgoing shortwave radiation in clear skies. As the reflectance of the shortwave radiation, outgoing shortwave has an almost linear relationship with the incoming shortwave. Generally, the outgoing shortwave, has the same tendency as the incoming shortwave. The value rises up in the morning and the peak moments happened in the noon for both of the days, around 60 $Wm^{-2}$.

Table 3.4 outgoing shortwave radiation average difference and peak information of clear skies

| Time(Julian DOY) | Peak time(Julian DOY) | | Peak value ( $Wm^{-2}$ ) | | Average difference of daytime ( $Wm^{-2}$ ) |
|---|---|---|---|---|---|
| | CNR1 | CNR4 | CNR1 | CNR4 | |
| 290 (clear) | 290.5 | 290.5 | 47 | 63 | -13.2 |
| 297 (clear) | 297.5 | 297.5 | 41 | 59 | -9.3 |

For the difference between the two sensors (CNR1 and CNR4) is completely different for outgoing radiation. The value of CNR1 is lower than the CNR4 over the whole study period. The average difference -13 $Wm^{-2}$ DOY 290 and -9.3 $Wm^{-2}$ in DOY 297 shown the downward-facing sensor on CNR4 received more reflectance from the tower. The largest contamination effects happened when the difference is about 19 $Wm^{-2}$ in DOY 290.5 and 21 $Wm^{-2}$ in DOY 297.6 (the spike on DOY 297 is excluded). Considering that the surround canopy is much lower than the CNR1 and CNR4 position, the extra reflectance was mainly caused by the tower effects.

In clear skies, the tower contamination effects have a slight influence on the incoming shortwave radiation results. The average difference of incoming radiation were 15 $Wm^{-2}$ for DOY 290 and 9.6 $Wm^{-2}$ for DOY 297, the CNR1 results were approximately up to 10 % higher than CNR 4 results over the study period after eliminate spurious errors where could arise by incidental shading of instruments.

For outgoing shortwave, the tower have an impactful effects to the measurement results. After removing the abnormal noisy existed in the midday of DOY 297, the CNR1 results were approximately 40% lower than CNR 4 results over the clear skies.

Compared to clear skies, the result of cloudy sky shown the incoming and outgoing radiation have a huge difference.

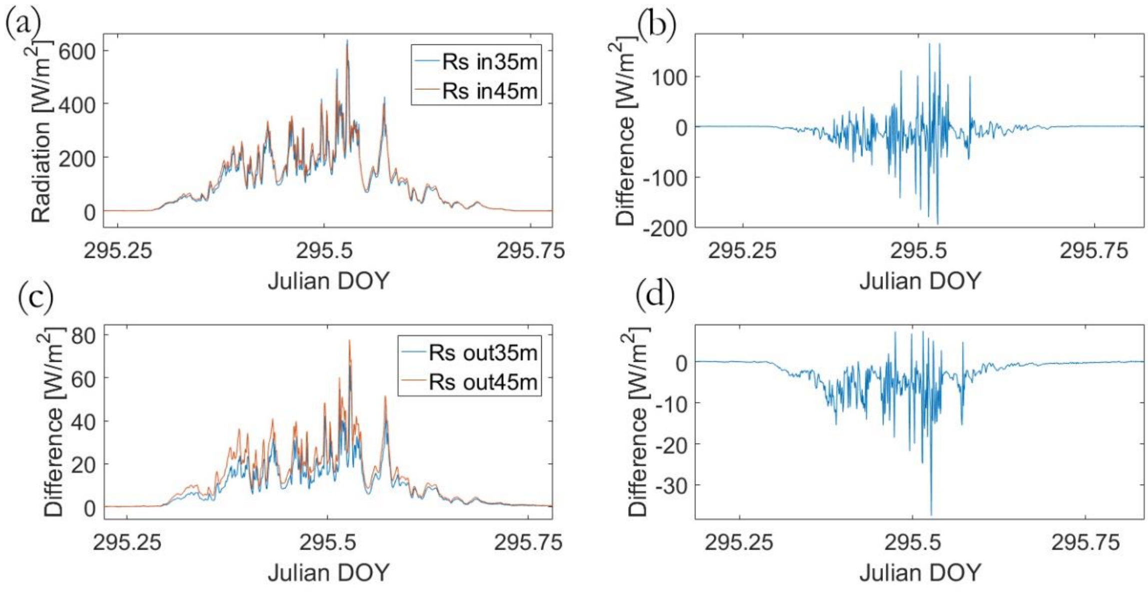


Figure 3.6 comparison and differences of shortwave radiation in cloudy sky (a) comparison of incoming shortwave radiation (b) differences of incoming shortwave radiation (c) comparison of outgoing shortwave radiation (d) differences of outgoing shortwave radiation.

Figure 3.7 shows the incoming and outgoing radiation and difference under a typical cloudy sky. The incoming radiation started rising up after the sun rise. As the time went on, the frequent and intense fluctuation occurred till the end of the day. The similar pattern display for outgoing shortwave radiation in cloudy sky, observed data was under very unstable situation.

Table 3.5 shortwave radiation average difference and peak information of overcast condition

| Time(Julian DOY) | Peak time(Julian DOY) | | Peak value ($Wm^{-2}$) | | Average difference of daytime ( $Wm^{-2}$) |
|---|---|---|---|---|---|
| | CNR1 | CNR4 | CNR1 | CNR4 | |
| Incoming in 295 | 295.5 | 290.5 | 47 | 63 | -10.3 |
| Outgoing in 295 | 295.5 | 297.5 | 41 | 59 | -4.1 |

The huge amount of fluctuations and the range of amplitude shows that when the radiative conditions was under partially clouded conditions there was no consistency and tendency in these fluctuations. Based on the meteorological data, the incoming radiation transmission was influenced by a large body of cover which caused the diffusion in the sky and continuously stable illumination, the radiation fell into irregularly reflection in the sky. The instruments kept receiving the radiation from all direction.

### 3.2.2. Temporal variability and tower contamination of longwave radiation

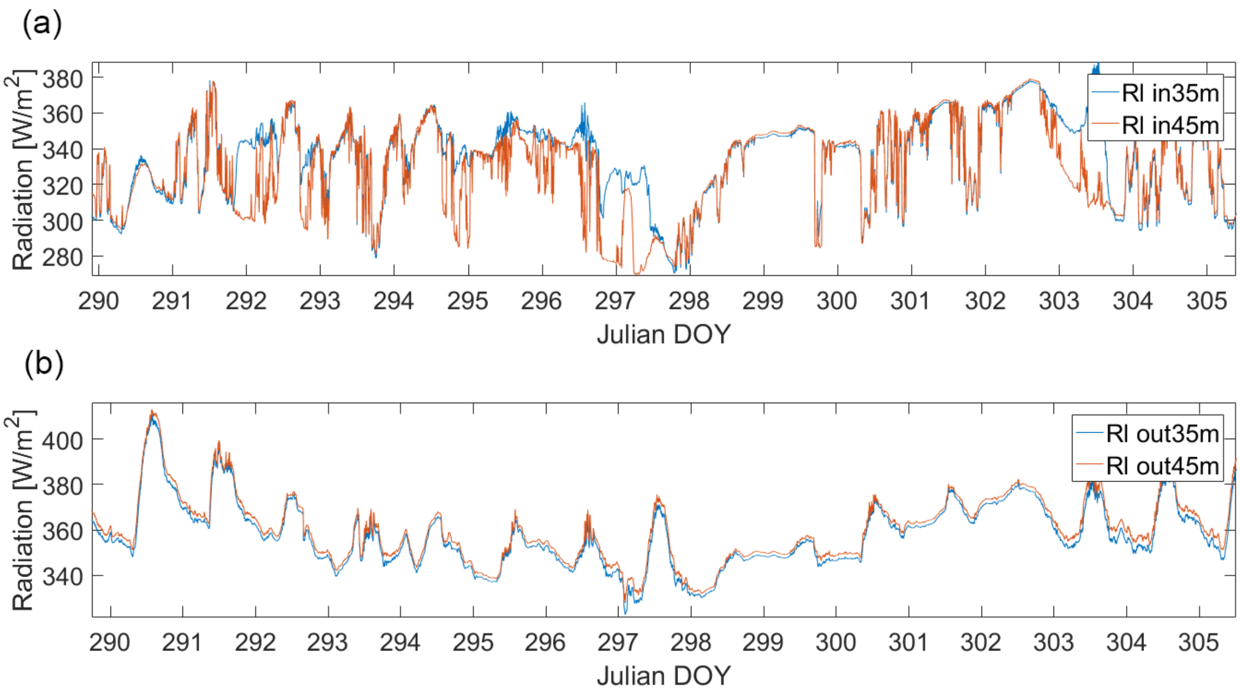


Figure 3.7 the comparison of diurnal variation of longwave radiation from DOY 290 to 305 in 2016. (a) The variation of incoming longwave radiation. (b) The variation of outgoing longwave radiation.

Figure 3.8 shows the diurnal variation of longwave radiation over the study period. In clear skies, there were no consistency or the same tendency of incoming longwave radiation. Due to the source of incoming longwave as the emitted radiation from the skies and clouds, during the whole study period the incoming longwave radiation were continually reaching the sensor over day and night, so the amount of the radiation flux shows the irregularly fluctuation sustained. For mostly of the time, the incoming radiation detected by CNR1 is higher than CNR4.

Compared with irregularly incoming longwave radiation, the outgoing longwave radiation have a difference performance. The peaks for outgoing radiation occurs in the middle of day for each days. The increase occurs around sunrise, decreasing of outgoing radiation occurs in the afternoon. The land absorption from incoming radiation emitted was the main factor that affects the near-surface diurnal outgoing longwave variability. Based on the results, CNR4 collected more outgoing radiations to CNR1 over the study period.

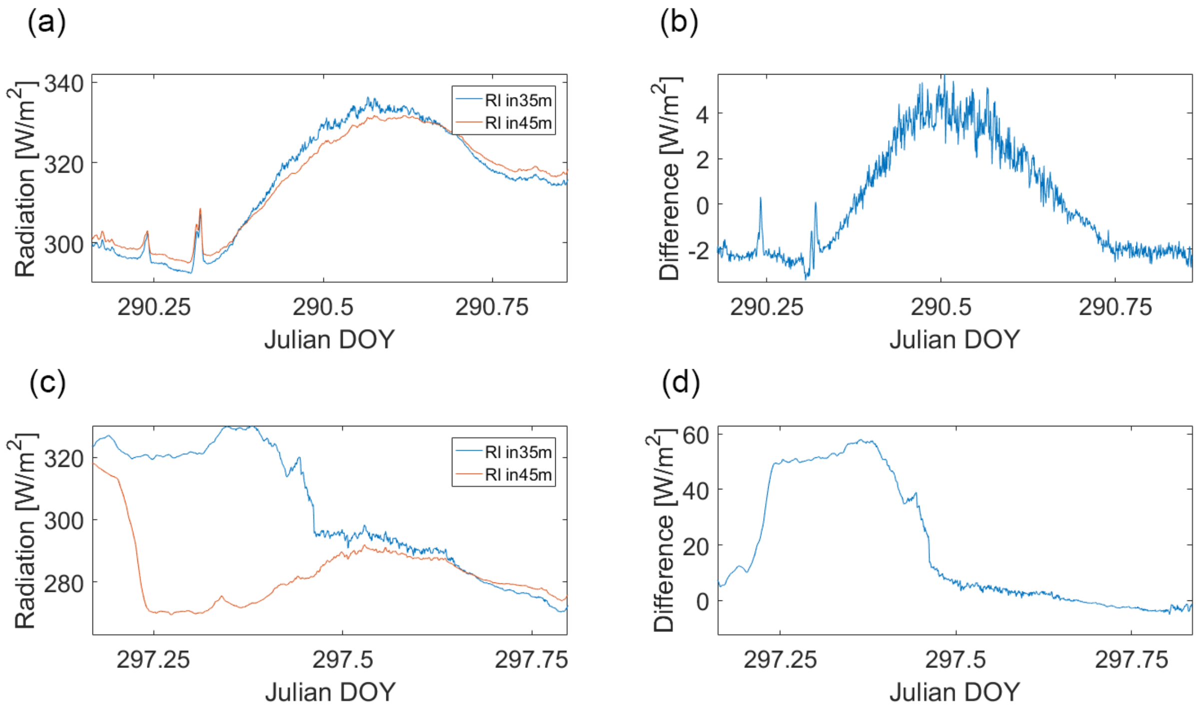

Figure 3.8 comparison and differences of incoming shortwave radiation in clear-skies (a) comparison of incoming shortwave radiation DOY 290 (b) differences of incoming shortwave radiation in DOY 290 (c) comparison of incoming shortwave radiation DOY 297 (d) differences of incoming shortwave radiation in DOY 297

Table 3.6 incoming longwave radiation average difference and peak information of clear skies

| Time(Julian DOY) | Peak time(Julian DOY) | | Peak value (Wm-2) | | Average difference of daytime(Wm-2) |
|---|---|---|---|---|---|
| | CNR1 | CNR4 | CNR1 | CNR4 | |
| 290 (clear) | 290.54 | 290.56 | 336.5 | 331.5 | 1.6 |
| 297 (clear) | 297.55 | 297.17 | 330.76 | 318 | 23.3 |

The variation of incoming longwave radiation of DOY 290 and 297 shows in Figure 3.9. As the longwave radiation is a function of emissivity and temperature. The incoming radiation increased round 8:00 in the morning (DOY 290.25) and the peak moments is on the afternoon. However, in the Figure 3.9(c), DOY 297, the radiation detected by CNR1 and CNR4 shows a different shape. The huge difference occurred around DOY 297.1, the radiation reached was increased for CNR1 but decreased for CNR4. As the consistency between net radiometers have been proved, and the incoming shortwave shows the upward sensor was not shadowed, thus the strange appearance in the morning in DOY 297 may be resulted of miscalculation by net radiometer system itself.

For a typical clear sky, DOY 290, the average difference was around 1.6 $Wm^{-2}$ while the range of incoming longwave radiation is between 280 and 340 $Wm^{-2}$ in DOY 290. The difference indicated the tower contamination to the net radiometers measurement result is quite small.

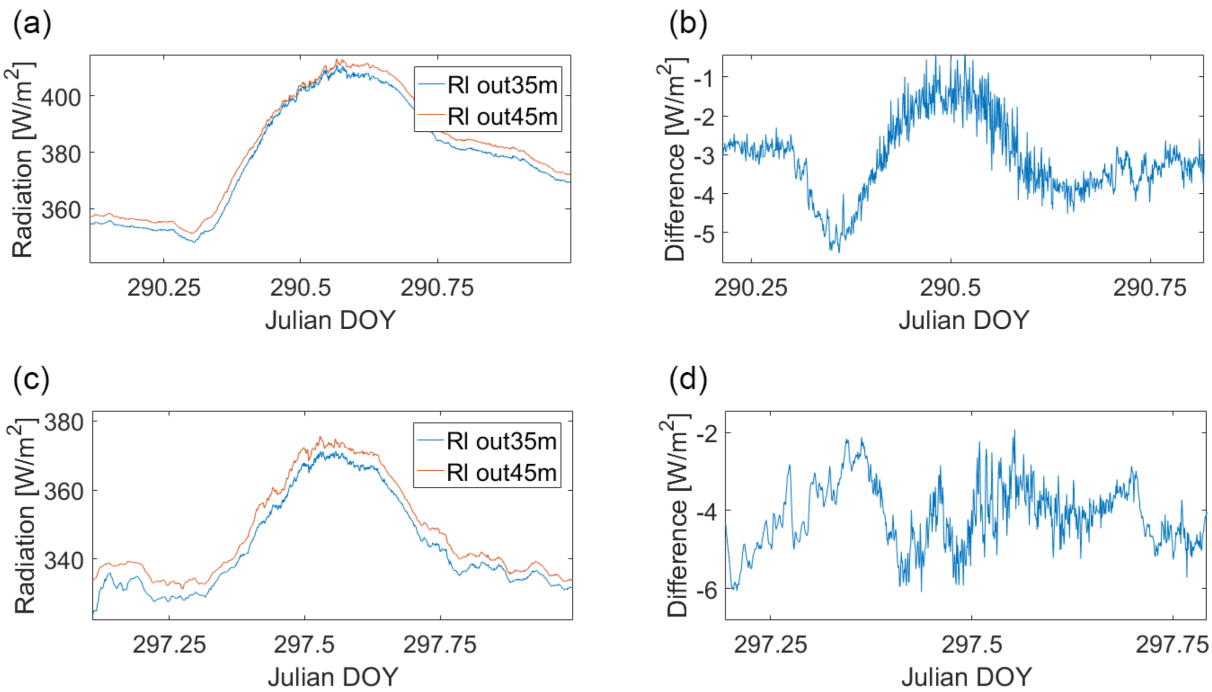


Figure 3.9 Plot the outgoing longwave in height of 35 meter and 45 meter in different days. (a) longwave in DOY 290. (b) longwave in DOY 290. (c) Difference of outgoing longwave in DOY 297. (d) Difference of outgoing longwave in DOY 297.

Table 3.7 outgoing longwave radiation average difference and peak information of clear skies

| Time(Julian DOY) | Peak time(Julian DOY) | | Peak value (Wm-2) | | Average difference of daytime(Wm-2) |
|---|---|---|---|---|---|
| | CNR1 | CNR4 | CNR1 | CNR4 | |
| 290 (clear) | 290.56 | 290.56 | 411 | 413 | -3.0757 |
| 297 (clear) | 297.53 | 297.53 | 371 | 375.5 | -3.9238 |

The Figure 3.10 shows the outgoing longwave radiation in clear sky, DOY 290 and 297, the curves was no longer as irregularly as the incoming radiation.

The outgoing longwave radiation, as the reflected radiation from the air and sky emitted by the solar radiation absorption, it has a similar performance as the solar radiation. The radiation rises after sunrise, and peaks occurred in DOY 290.56 and 297.53 of each day. Then the value started decreased, approached the value in the morning. The outgoing radiation is highly related to the temperature, as land has been heated by the solar, the temperature rise up at the same time, than the outgoing radiation became larger. Most of the radiation came from the downward of the tower, then tower reflection was the mainly effected factor contributing the difference. The difference change in a very small range. The average difference was 3 $Wm^{-2}$ in DOY 290 and -4 $Wm^{-2}$ in DOY 297.The highest value was about 5 $Wm^{-2}$ in DOY 290 when the outgoing radiation was about 370 $Wm^{-2}$ in the morning and 6 $Wm^{-2}$ in DOY 297 while the CNR1 and CNR4 measurement value reached to 320 $Wm^{-2}$.

The outgoing radiation was captured by downward sensors, field of view about 180°. As the CNR4 was 10 meters higher than the CNR1, the downward sensors on the CNR4 detected a larger reflected radiations. Based on the results, under the clear skies, the tower body just have a slightly impaction on the measurement result, up to 2% in total.

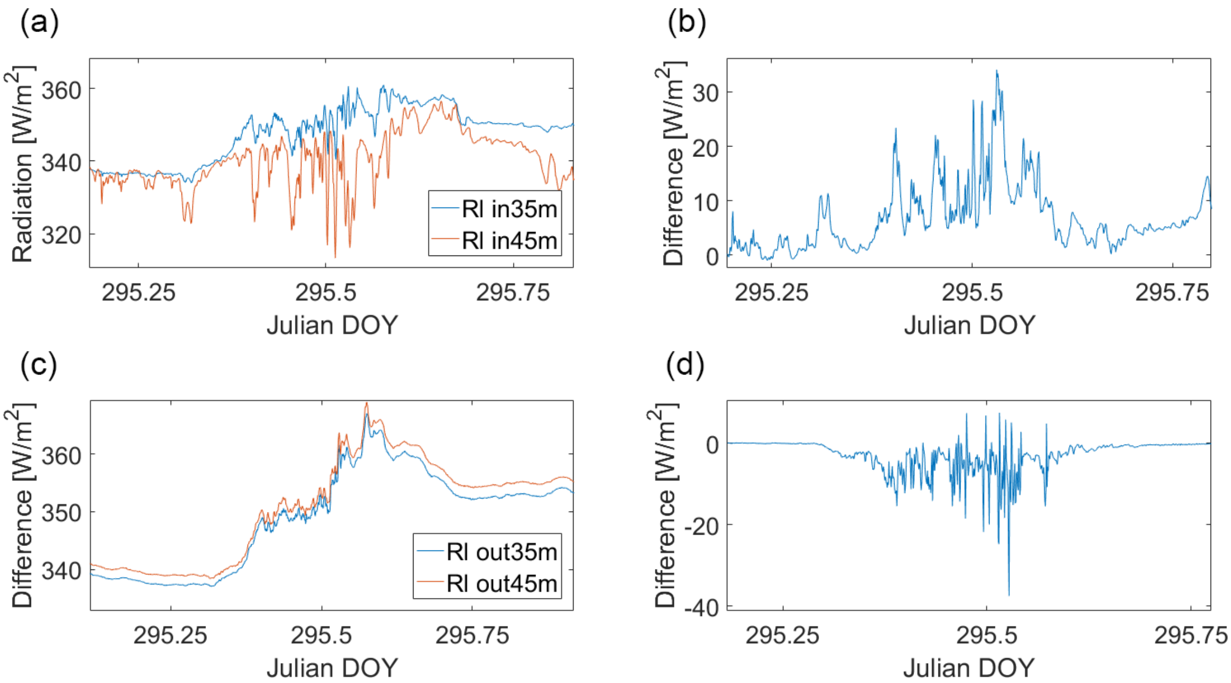


Figure 3.10 (a) Incoming longwave. (b) Difference of incoming longwave. (c) Outgoing longwave. (d) Difference of outgoing longwave.

Figure 3.11 shows the incoming and outgoing longwave in cloudy sky. The result show for incoming longwave, the CNR1 variation results remain in an stable performance, fluctuating between the 340 and 360 $Wm^{-2}$, at the same time; the CNR4 results varies between 310 and 350 $Wm^{-2}$. The average difference during the day time was about 8.44 $Wm^{-2}$, compared with the total amount of radiation, the difference indicated the under the cloudy sky situation, the radiation reached both instruments was analogically. The highest difference was 38 $Wm^{-2}$ while the CNR 1 was approximately 350 $Wm^{-2}$. It shows the tower contamination effects to the result in a small radiation level.

Table 3.8 longwave radiation average difference and peak information of overcast condition

| Time(Julian DOY) | Peak time (Julian DOY) | | Peak value ($Wm^{-2}$) | | Average difference of daytime ($Wm^{-2}$) |
|---|---|---|---|---|---|
| | CNR1 | CNR4 | CNR1 | CNR4 | |
| Incoming in 295 | 295.58 | 295.65 | 361 | 356 | 8.4 |
| Outgoing in 295 | 295.57 | 297.57 | 367 | 369 | -1.6 |

As the previously result, the outgoing radiation in cloudy sky was quite similar with the clear sky. The CNR4 result was higher than the CNR1 during the day and the peak moment happened around 13:00 hr

(DOY 297.57). Although the difference value continue changing between the positive and negative value, the difference still remained in a small level. The average difference was around 1.6 $Wm^{-2}$ during the day time while the measurement value fluctuating between 335 and 370 $Wm^{-2}$ for both of the instruments. And the highest difference was around 38 $Wm^{-2}$, occurred in the afternoon while the radiation reached the peak, 370 $Wm^{-2}$. In spite of the influence from the tower, the two instruments result still remained a good consistency, difference of result up to 9%.
As a series of day time longwave radiation and there difference between the CNR1 and CNR4 been quantified, after removing the time period with remarkable instruments measurement errors, the measurement result from the CNR1 and CNR4 indicate the incoming and outgoing radiation under all – sky condition have a slightly impact from the reflection of the tower body during the diurnal longwave radiation variation.

### 3.2.3. Temporal variability and Net radiation

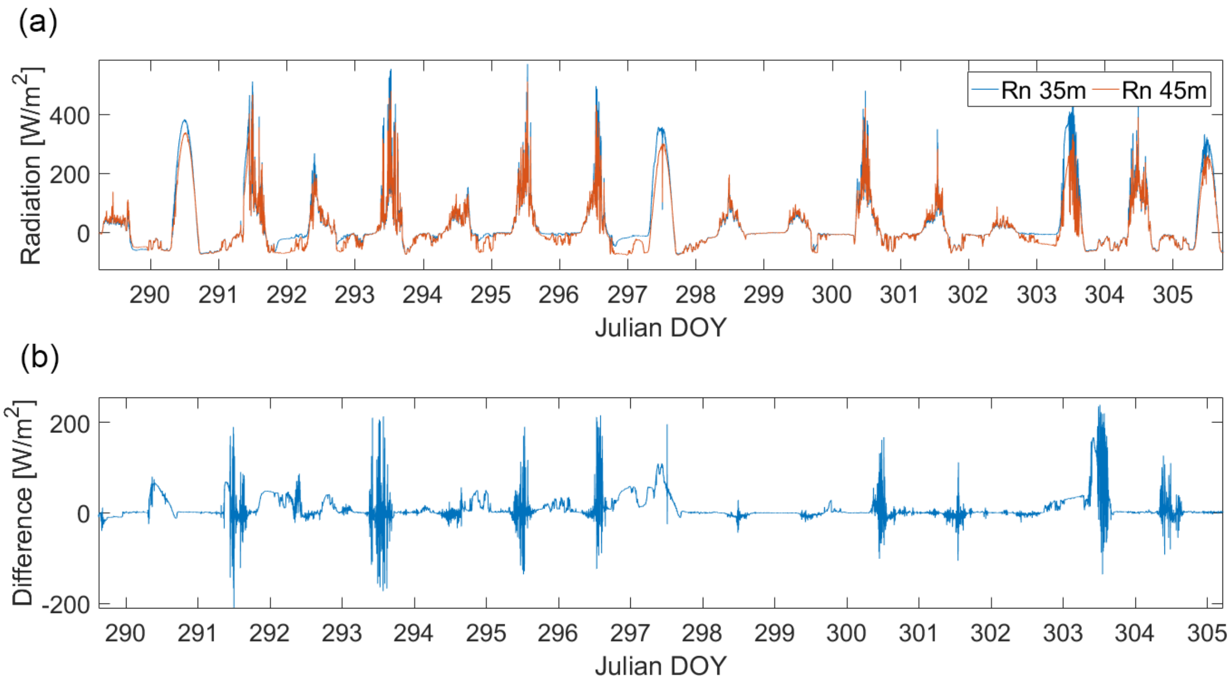


Figure 3.11 (a) Net radiation in 35 meters and 45 meters height during measurement period. (b) Difference in 35 meters and 45 meters of net radiation.

The Figure 3.12 shows the diurnal variation of net radiation during the study period. The net radiation was the sum of total shortwave and longwave. In the night time, the radiation value remained relatively stable situation which were between -70 to 0 $Wm^{-2}$, because there were no solar radiation at night, the longwave is the mainly component of net radiation. During the day time, the changing of incoming shortwave radiation contributed most for the diurnal radiation variation. To some extent, the variation of net radiation has a similar characteristic to the incoming shortwave radiation.
The net radiation in different weather condition have different performance. For clear skies, the curves of net radiation were more smoothly for the incoming radiation directly reaching the sensors, no cloudy disturbed, peak values normally occurred in the noon, around 380 $Wm^{-2}$. For cloudy skies, because the

emission of the solar radiation absorbed by the cloud, the curves shows very unstable and severely changing during the day, the highest value was about 600 $Wm^{-2}$ and the time of peak occurred irregularly.

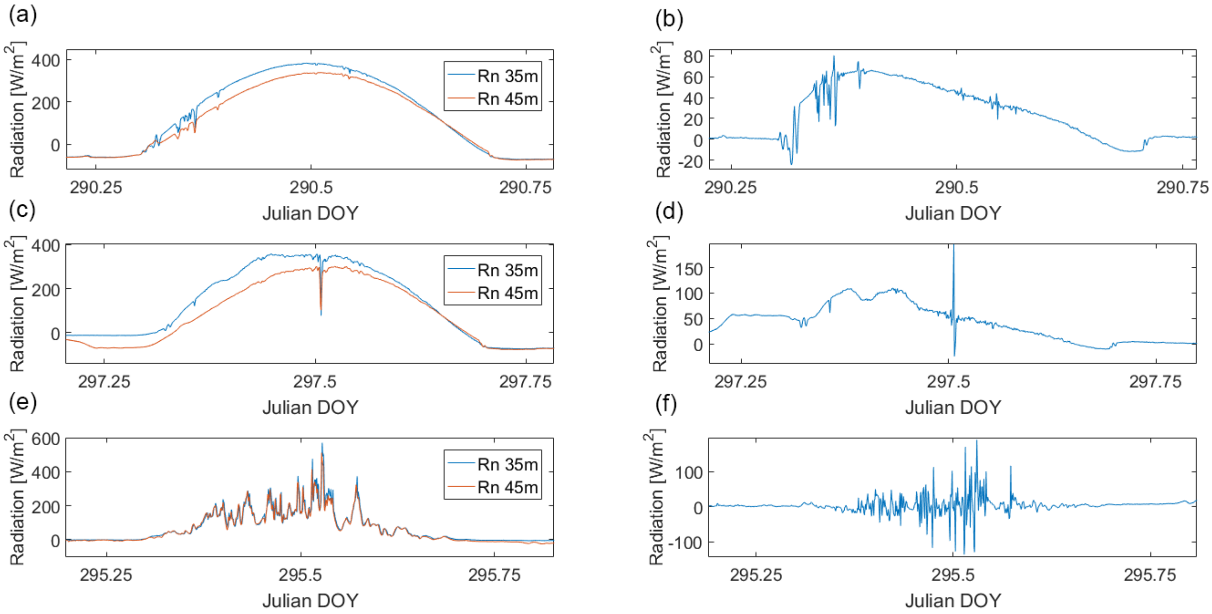


Figure 3.12 diurnal net radiation variation in all skies condition

Table 3.9 net radiation average difference and peak information in all sky condition

| Time(Julian DOY) | Peak time(Julian DOY) | | Peak value ($Wm^{-2}$) | | Average difference of daytime ($Wm^{-2}$) |
|---|---|---|---|---|---|
| | CNR1 | CNR4 | CNR1 | CNR4 | |
| 290 (clear) | 290.56 | 290.56 | 380 | 336 | 32.6 |
| 297 (clear) | 297.5 | 297.5 | 360 | 300 | 49.9 |
| 295 (cloudy) | 295.6 | 295.6 | 571 | 510 | 3.8 |

Figure 3.13 shows the diurnal net radiation variation in all skies condition. Due to the longwave uncertainty, net radiation variability is large on some parts of DOY 290 and 295.

In clear sky, the net radiation remained in steady value before the sun rise, there was -60 $Wm^{-2}$ in DOY 290. During that time, the difference was 0 $Wm^{-2}$ which indicated that the two instruments results have a great consistency, there was no incoming solar radiation, thus the longwave radiation was the only source for net radiation. Net radiation rose after sunrise. At the same time, the divergence between the two sensors described earlier occurs. The variation of solar radiation began occupying the dominant position in net radiation variability. Also, since the incoming solar radiation was highly affected by the tower body reflection, tower was the main factor contributing to the divergence. The average difference of DOY was 32 $Wm^{-2}$ during the day time and highest difference occurred in the morning while the net radiation was 220 $Wm^{-2}$ for CNR1 and 160 $Wm^{-2}$ for CNR4. The peak moments was in the mid time of the day. Then the value started gradually decreasing to -60 $Wm^{-2}$, almost equal to the morning value.

For cloudy sky, the curve net radiation shows that before the sun rise, the longwave radiation contributed to the total radiation and remained a steady state as in the clear sky. As time went by, the curves started becoming irregularly and unsteady. Due to the diffuse solar radiation, the radiation kept strongly fluctuating and the peak was occurred in the afternoon, around 571 $Wm^{-2}$ for CNR1 and 510 $Wm^{-2}$ for CNR4.

The average difference of cloudy sky was about 3.8 $Wm^{-2}$. The small difference also happened in the longwave performance in previously part. The variation of longwave radiation was the determinant factor to the net radiation variability. The highest difference was almost 180 $Wm^{-2}$, occurred in the afternoon.

Under all sky conditions, compared with the CNR4 that on the top of the tower, CNR1 which is just 3 meters higher than the canopy, the tower reflected irradiance could leads the difference up to 50% (on outgoing shortwave measurement). In addition, incoming solar radiation and its reflected radiation variation are the main contributed factors to the diurnal net radiation cycle.
A remarkable performance also happened in comparison of net radiation in clear skies. The difference was larger in the morning and lower in the afternoon. The solar radiation variability was intimately linked to the net radiation variability, thus as the explanation in the previously section, the tower reflected-area in the front side may be considered to be responsible for this appearance.

#### 3.2.4. Dependency of incoming radiation difference and net radiation on SZA

The difference refer to the reflected radiation by tower body have been quantified. Furthermore, if the angle measured at the surface between the sun and zenith has contributed to the difference remains to be elucidated. The following figures shown relationship between the SZA and the difference of incoming shortwave radiation, net radiation measurement.

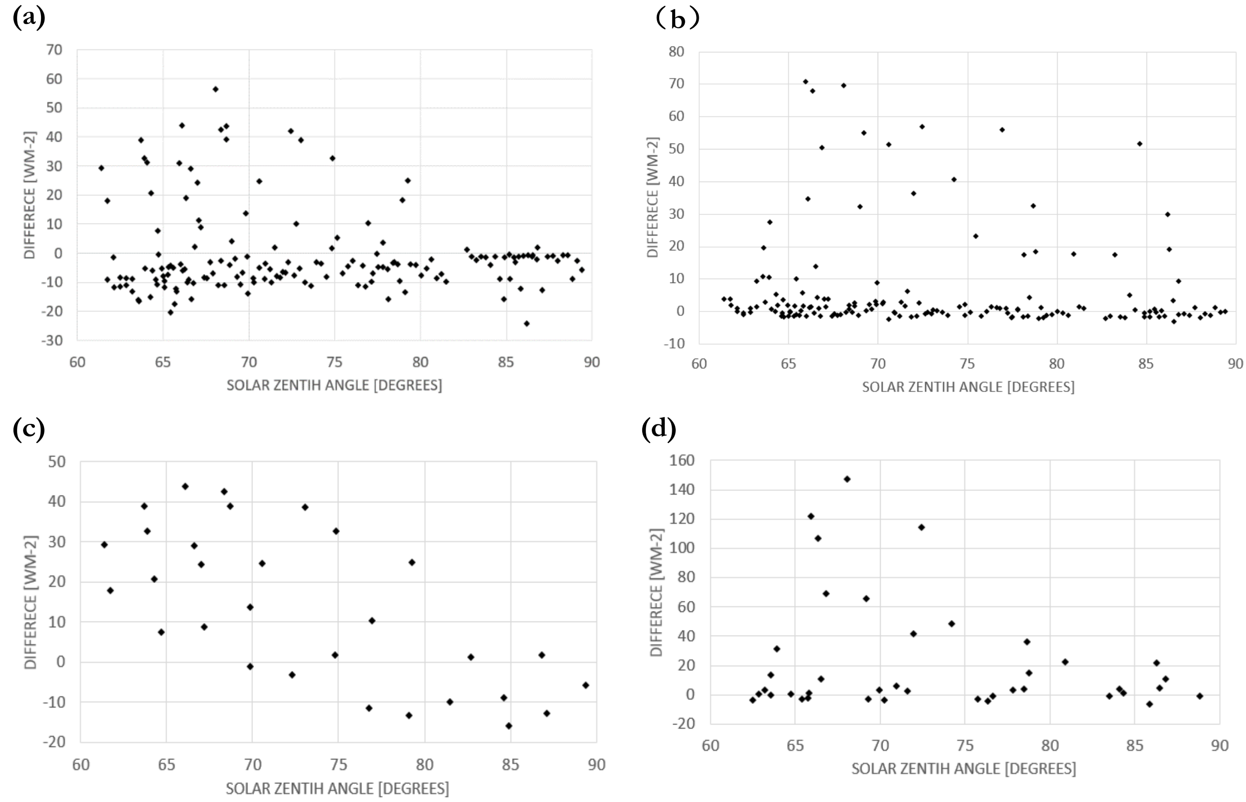


Figure 3.13 the relationship between the SZA and difference of radiations. (a) overview the difference of incoming radiation (b) overview the difference of net radiation (c) in clear skies, difference of incoming radiation (d) in clear skies, DOY 290, 297 and 303, difference of net radiation

Figure 3.13(a) shows under all skies condition, the relationship between the solar zenith angle and incoming shortwave radiation. There was a clear characteristic that most of the results concentrate among the range of -20 to 0 $Wm^{-2}$ when the solar zenith angle was from 60 to 90 degrees. A few of the results are in the range of 10 to 60 $Wm^{-2}$ while the degrees are smaller than 80 degrees. Figure 3.13(b) shows the relationship between the net radiation and solar zenith angle. Obviously a large amount of results located about 0 $Wm^{-2}$ in larger SZA. Because during this time, the sun close to sunset and sun rise, the density of solar radiation was quite small and rare radiation been reflected by the tower body.

It was clear that for most of time, no matter how the solar located, the fluctuation of difference could remained in low amplitude. With the solar zenith getting smaller, the difference start getting larger. Meanwhile, the high difference range existed while the solar zenith angle approach 60 degrees. The reason was while the SZA hold minor value, the sun located on the highest altitude, the reflected-area achieved intend to be the largest. Consequently, the CNR1 received the largest reflected radiation and caused the highest difference. Besides, it worth to mention that the highest difference occurred while the solar zenith angle approach to 68 degrees, but not the minimum 60 degrees. As the explanation in section 3.2.1, the possible reason may be caused by CNR1 installed position to the tower, closed to right cause the highest reflected radiation existed not in the noon, but a little advanced.

Figure 3.13(c) and (d) shown the solar zenith angle verse incoming solar radiation and net radiation under clear skies. Because of lack of enough clear skies, the difference of incoming solar radiation with SZA was not so remarkable, but it still can observed the characteristic that the largest difference existed when the SZA stay in 65 degrees. Meanwhile, with the SZA increased, the difference decreased.

Generally speaking, all those characteristics above indicated reflected radiation by the tower body could related to the SZA variation. The largest tower contamination effects to the net radiometers measurement occurred while the SZA kept minimum. At the same time, the tower contamination could get smaller if the SZA decreased.

### 3.3. Temporal variability of albedo

#### 3.3.1. The seasonal variability

The figure shows the radiation and albedo varied with growing season started at 27th February 2015 last 365 days.

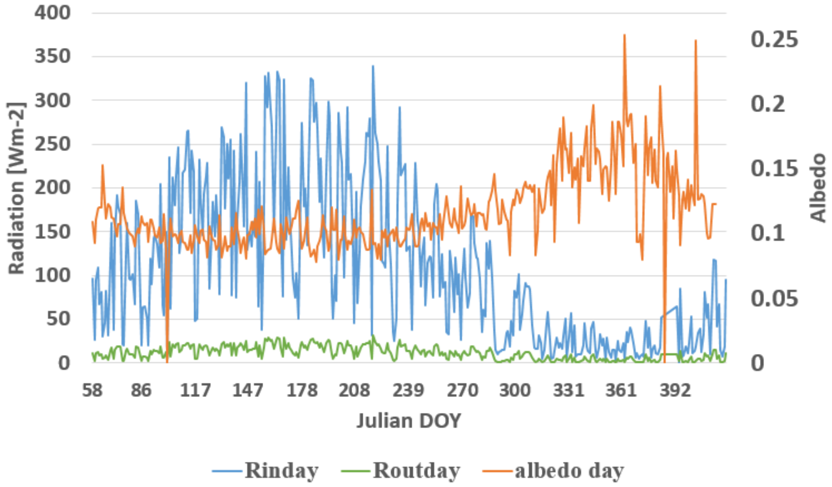


Figure 3.14 temporal variability of daily incoming and outgoing shortwave radiation and albedo.

The figure shown the variation of shortwave and albedo from DOY 58 in year 2015 till the same day in next year, recorded by CNR1 net radiometers. In this study mainly focusing on the albedo performance in clear skies.

Obviously, the daily solar radiation seasonal variability matched ideal radiation variation. Generally speaking, at the beginning of spring, DOY 58, 27th January 2015, both of daily incoming and outgoing shortwave were lower than in the summer time. The minimum incoming and outgoing radiation occurred in the winter of 2015. Then with the time went on, the daily incoming and outgoing radiation started increased again. Both of the trends of radiations along with severely fluctuation, the cloudy cover was treated as the mainly contributed reason. While the skies were covered by the cloud, the occasionally cloud trapped the incoming solar radiation from time to time, thus the average value between two adjacent days could have distinct difference.

The albedo a function of the reflectance of the soil and forest canopy and the fraction of reflected solar energy which should back to space, these may change during the season. The albedo during the study period shows a clear characteristic. In the spring of 2105, the albedo remained around 0.1. Then the albedo varied during the growing season, the albedo slightly decreased throughout the spring. The smallest albedo was around 0.07 occurred in the summer, DOY 184 (Excluded the albedo in DOY 100 which albedo was 0, not reasonable) while the largest volume of incoming radiation reached the measurement senor. Then with the decrease of incoming radiation, the albedo was gradually rising up. The albedo reached 0.25 once in the DOY 359, winter. For the rest of the days in winter, the mean albedo was changing around 0.15.In the winter, the albedo is much higher than summer time.

It is clear that clouds affect the incoming radiation. But the albedo as a property of the surface wouldn't be affected by the cloud variation in the sky. We speculated that since the study area is full of needle-leaved trees, the density of the canopy or the greenness remains the same during summer and winter, the changing of albedo may due to difference of the sun position in growing seasons.

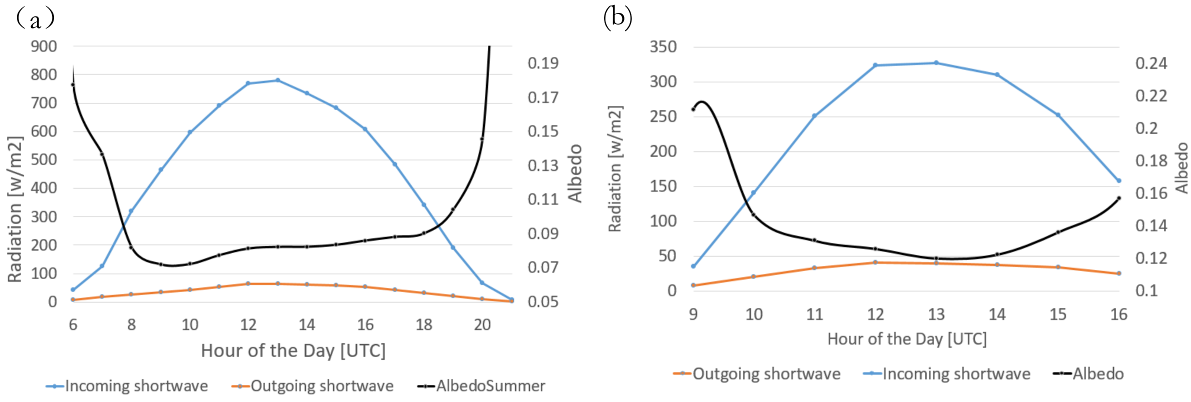


Figure 3.15 hourly mean value in (a) summer and (b) winter clear skies

The measurement been proceed under the clear skies were used to determine the variability of different energy patterns and the dependency of albedo on SZA.

The data been processed as the hour-to-hour data of each hour of the day via Matlab. The selection of clear skies were based on KNMI meteorology cloud cover index.

Figure 3.15 shows for both of summer and winter, the albedo have a "bowl" shape cycle with the highest albedo value occurred in the morning and later in the afternoon. Meanwhile Figure 3.15 (b) shows a clear symmetrical hourly albedo was around the local solar noon. Figure 3.16(a) shows the smallest albedo is 0.7 occurred at 9:00 hr in the morning, and the albedo sustained rise up till 0.9 at 18:00 hr. The winter albedo shows in the Figure 3.15(b) that albedo strongly varies during the diurnal albedo cycle. The smallest albedo occurred was 0.12 at 13:00 hr. The mean albedo during the day time in summer was 0.082 while in the winter was much higher, reaching 0.135.

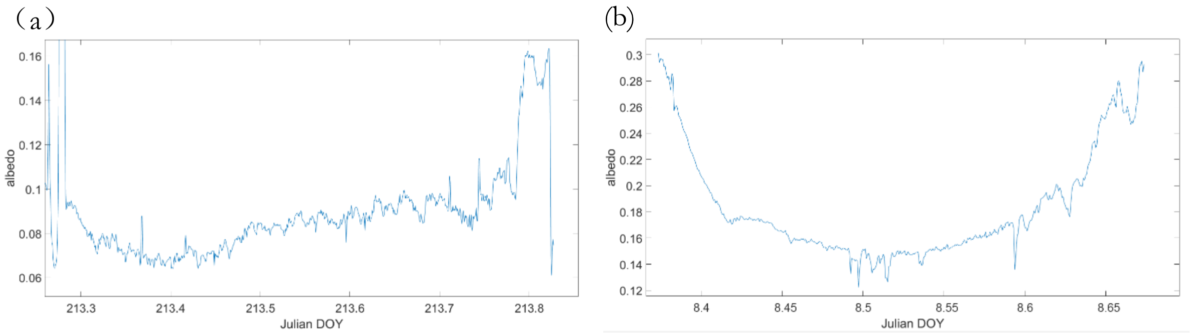


Figure 3.16 the diurnal albedo cycle

To be more specifically, two typical clear sky days, one is in summer (DOY 213 in 2015) and the other is in winter (DOY 8 in 2016) have been shown in Figure 3.16(a) and (b) respectively, which give more specific information for the diurnal variation of albedo. The distinctly elevation existed in the early morning and close to evening. With the time went on, the summer albedo kept changing in the range between 0.064 and 0.105 and lowest value occurred in the 10:00 hr (DOY 213.4). The amplitude of albedo in the DOY 8 in 2016 was larger, that the smallest albedo was 0.122 at noon and around 0.2 at the beginning and ending of the day time. There tendency of Figure 3.16 also highly matched with Figure

3.15, during the summer, the albedo was more smoothly, proved the albedo in the winter was more sensitive to the hour of day.

Overall, the diurnal change of the albedo is consistent with the results of previous studies(Weligepolage, Gieske, and Su 2013) for green ever forest in high latitude, which presents nearly a "U" shape with highest value of albedo in the morning and later one in the afternoon. On the other hand, there exists significant difference of the albedo variation between summer and winter, which may be attributed to the SZA presented in the following section.

#### 3.3.2. Dependency of albedo and solar radiation difference on SZA

SZA plays an important role in the diurnal variation of albedo. In order to figure out the relationship between SZA and the variation of albedo in our study area, we select the albedo in clear skies in summer and winter, which display in Figure 3.16. It can be seen that there is a clear difference of albedo associating with the change of SZA. For instance, in winter, while the incidence solar radiation change close to zenith, the smallest degrees was 30° and 65°. One should be mentioned here is that in summer when SZA is higher than 65°, the albedo has obvious variation, in contrast, in winter, this phenomenon appears with the SZA exceeding 75°. In addition, it can be found that most of the values concentrate under 0.1 and remain steady with the change of SZA from 30° to 65° in summer, while the value of albedo verse SZA in the winter remain 0.11 with the SZA changing from 65° to 73°.

The "bowl" shape albedo performance not only appeared in the hour-to-hour albedo performance but also in the daily diurnal albedo cycle averaged in 1 minute, the same pattern shape also been mention by other researchers(Lafleur, Wurtele, and Duguay 1997; Ross 2012). The albedo in the forest was highly related to the SZA that the increasing of SZA leads the increasing in albedo. The possible reason may be caused by the incidence solar radiation. Different incidence angle leads different result. Compared to the solar radiation incidence from the zenith, while the incidence angle closes to the horizon a large volume of solar radiation have been scattered by the upper canopy.

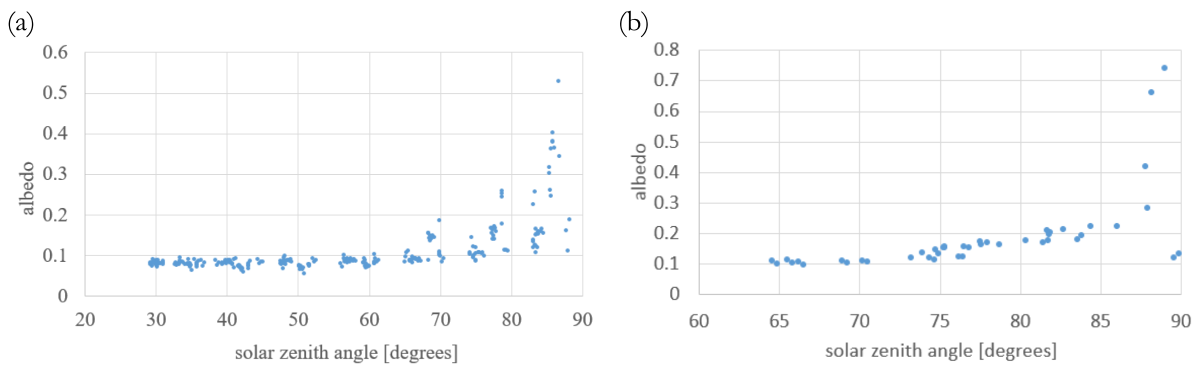


Figure 3.17 dependencies of albedo on SZA in (a) summer clear skies (b) winter

Moreover, the SZA may not be the only factor responsible for the higher albedo value in the winter. In some cases, the snow would also leads the uprise of albedo. Meanwhile, (Kuusinen et al. 2012)indicated sometimes the albedo value increased after snowfall without any new snow. This increase normally along with clear skies, which was largely correlated with high albedo while the snow covering the canopy.

Unfortunately, due to the rarely snow falling in Netherlands, we cannot acquire adequate data for doing the testing.

# 4. CONCLUSION

This study mainly concentrates on the diurnal temporal variability and the error from tower-based measurement in different types of radiations in Douglar fir forest, as well as albedo. We use the radiation observation data obtained from the tower station from 27th February 2015 to 27th February 2016. The tower locates in the area of ( $52^{\circ}05'08.1"N,\ 5^{\circ}41'25.8"E$) installing with the two types of net radiometers, namely CNR1 and CNR4, which had been installed at 35 meters and 45 meters of the measurement tower respectively. These two net radiometers have homogenous surroundings and underlying surface.

First of all, in order to verify the reliability of our measuring datasets, we made an experiment for valuing the tower contamination. We installed the same instruments in the garden of ITC for discovering the instruments consistency and original difference between CNR1 and CNR4. The results prove a well consistency of two instruments: without the irregular incoming radiation caused by sky diffusion and r-squared were greater than 0.98.

Based on the previously results, we are able to conclude the tower contamination effects can't be ignored. The difference was up to 7% compared with original difference in the incoming shortwave measurement For outgoing shortwave radiation measurement, the results indicated the tower have largely influenced the outgoing radiation measurement, The CNR4 results were approximately up to 23.2% higher than the CNR1 results. But for the longwave measurement, all the results show the tower contamination effects are quite small that the difference caused by reflected are under 2%. The net radiation measurement is not precisely enough. On the one hand, the difference could reach 50% between the two instruments. On the other hand, the reflected radiation should be responsible for the huge discrepancy.

We can speculate if the highly precisely radiation data is needed, radiation still need to be corrected even only using the net radiometers on the top of the tower.

Moreover, the SZA contributes to the difference in all types of radiations measurements. During the study period, the highest difference occurs while the solar is closest to the zenith. Meanwhile with the decrease of SZA the difference decrease as well.

The albedo variability over seasons shows the in the morning and afternoon, a large portion of incoming radiation will be reflected back to space. For the seasonal cycle, the albedo in the summer is lower than winter in the clear skies. Since the needle-leaved forest is the only species in the study area, the seasonal change of the greenness cloud be ignored. The SZA was treated as the main factor influenced the albedo temporal variability. When the solar close to the zenith, the albedo have the minimum value in either summer or winter. The smallest SZA in the summer and winter proved the solar position is trigger the changing of albedo value. The albedo increased with SZA increased. Meanwhile also the SZA is highly related with albedo, it is not strongly varied with albedo when the SZA is less than 65 degrees.

The study indicated the radiation temporal variability in diurnal cycle and tower-based measurement contamination effects to the results, as well as albedo. In addition, it has been proved that the solar zenith angle could influenced the tower-based contamination and the temporal variability of albedo in a needle-leaved forest. This study would be more accurately if we can collected more data from the in-situ measurement.

# REFERENCES


Amiro, BD, and SC Sheppard. 1994. 'Effects of ionizing radiation on the boreal forest: Canada's FIG experiment, with implications for radionuclides', *Science of the total environment*, 157: 371-82.

Bastable, HG, William J Shuttleworth, RLG Dallarosa, G Fisch, and Carlos A Nobre. 1993. 'Observations of climate, albedo, and surface radiation over cleared and undisturbed Amazonian forest', *International Journal of Climatology*, 13: 783-96.

Betts, Alan K, and John H Ball. 1997. 'Albedo over the boreal forest', *Journal of Geophysical Research: Atmospheres*, 102: 28901-09.

Blonquist, JM, BD Tanner, and Bruce Bugbee. 2009. 'Evaluation of measurement accuracy and comparison of two new and three traditional net radiometers', *Agricultural and Forest Meteorology*, 149: 1709-21.

Chai, Tianfeng, and Roland R Draxler. 2014. 'Root mean square error (RMSE) or mean absolute error (MAE)?–Arguments against avoiding RMSE in the literature', *Geoscientific Model Development*, 7: 1247-50.

Dou, Baocheng, Jianguang Wen, Xiuhong Li, Qiang Liu, Qing Xiao, Junhua Bai, Jingjing Peng, Xingwen Lin, Zhigang Zhang, and Xiaodan Wu. 2015. "Sensor intercomparison of distributed surface radiation measurement system." In *International Conference on Intelligent Earth Observing and Applications*, 98081F-81F-6. International Society for Optics and Photonics.

Gardner, JL, and TP Jones. 1980. 'Multi-wavelength radiation pyrometry where reflectance is measured to estimate emissivity', *Journal of Physics E: Scientific Instruments*, 13: 306.

Gavilán, Pedro. 2016. 'Comparing Net Radiation Measurements Using Domeless and Domed Net Radiometers: Impact on ET o Estimations', *Journal of Irrigation and Drainage Engineering*, 142: 04016060.

Gavilan, Pedro, Joaquin Berengena, and Richard G Allen. 2007. 'Measuring versus estimating net radiation and soil heat flux: Impact on Penman–Monteith reference ET estimates in semiarid regions', *Agricultural Water Management*, 89: 275-86.

Ghatak, Debjani, Eric Sinsky, and James Miller. 2014. 'Role of snow-albedo feedback in higher elevation warming over the Himalayas, Tibetan Plateau and Central Asia', *Environmental Research Letters*, 9: 114008.

Guan, Xiaodan, Jianping Huang, Ni Guo, Jianrong Bi, and Guoyin Wang. 2009. 'Variability of soil moisture and its relationship with surface albedo and soil thermal parameters over the Loess Plateau', *Advances in Atmospheric Sciences*, 26: 692-700.

Houldcroft, Caroline J, William MF Grey, Mike Barnsley, Christopher M Taylor, Sietse O Los, and Peter RJ North. 2009. 'New vegetation albedo parameters and global fields of soil background albedo derived from MODIS for use in a climate model', *Journal of Hydrometeorology*, 10: 183-98.

Ide, Reiko, Yasuo Hirose, Hiroyuki Oguma, and Nobuko Saigusa. 2016. 'Development of a masking device to exclude contaminated reflection during tower-based measurements of spectral reflectance from a vegetation canopy', *Agricultural and Forest Meteorology*, 223: 141-50.

Khan, A, BS Nahar, MM Hossain, and MA Baten. 2015. 'Micrometeorological Parameter and Energy Balance over Soybean', *Journal of Environmental Science and Natural Resources*, 7: 69-74.

Kuusinen, Nea, Pasi Kolari, Janne Levula, Albert Porcar-Castell, Pauline Stenberg, and Frank Berninger. 2012. 'Seasonal variation in boreal pine forest albedo and effects of canopy snow on forest reflectance', *Agricultural and Forest Meteorology*, 164: 53-60.

Ladner, SD, R Arnone, R Vandermeulen, P Martinolich, A Lawson, J Bowers, R Crout, M Ondrusek, and G Fargion. 2014. "Inter-satellite comparison and evaluation of Navy SNPP VIIRS and MODIS-Aqua ocean color properties." In *SPIE Sensing Technology+ Applications*, 911107-07-9. International Society for Optics and Photonics.

Lafleur, Peter M, A Bruce Wurtele, and Claude R Duguay. 1997. 'Spatial and temporal variations in surface albedo of a subarctic landscape using surface-based measurements and remote sensing', *Arctic and Alpine Research*: 261-69.

Lee, Wei-Liang, KN Liou, Cenlin He, Hsin-Chien Liang, Tai-Chi Wang, Qinbin Li, Zhenxin Liu, and Qing Yue. 2016. 'Impact of absorbing aerosol deposition on snow albedo reduction over the southern Tibetan plateau based on satellite observations', *Theoretical and Applied Climatology*: 1-10.

Liang, Mei, Bojun Sun, Xiaogang Sun, and Junyan Xie. 2017. 'Development of a new fiber-optic multi-target multispectral pyrometer for achievable true temperature measurement of the solid rocket motor plume', *Measurement*, 95: 239-45.

Liu, Huizhi, Baomin Wang, and Congbin Fu. 2008. 'Relationships between surface albedo, soil thermal parameters and soil moisture in the semi-arid area of Tongyu, northeastern China', *Advances in Atmospheric Sciences*, 25: 757-64.

MacDonell, Shelley, Lindsey Nicholson, and Christophe Kinnard. 2013. 'Parameterisation of incoming longwave radiation over glacier surfaces in the semiarid Andes of Chile', *Theoretical and Applied Climatology*, 111: 513-28.

MacWhorter, MA, and RA Weller. 1991. 'Error in measurements of incoming shortwave radiation made from ships and buoys', *Journal of Atmospheric and Oceanic Technology*, 8: 108-17.

Manara, J, M Zipf, T Stark, M Arduini, H-P Ebert, A Tutschke, A Hallam, J Hanspal, M Langley, and J Hartmann. 2016. 'Development and Validation of a Long Wavelength Infrared (LWIR) Radiation Thermometer for Contactless Temperature Measurements in Gas Turbines During Operation'.

Monteith, JL, and G Szeicz. 1961. 'The radiation balance of bare soil and vegetation', *Quarterly Journal of the Royal Meteorological Society*, 87: 159-70.

Noi, Phan Thanh, Martin Kappas, and Jan Degener. 2016. 'Estimating Daily Maximum and Minimum Land Air Surface Temperature Using MODIS Land Surface Temperature Data and Ground Truth Data in Northern Vietnam', *Remote Sensing*, 8: 1002.

Pedersen, Leif Toudal, Rasmus T Tonboe, Jacob Høyer, and Roberto Saldo. 2016. "An optimal estimation algorithm to derive Ice and Ocean parameters from AMSR Microwave radiometer observations." In *ESA Living Planet Symposium 2016*.

Peng, Jingjing, Wenjie Fan, Xiru Xu, Lizhao Wang, Qinhuo Liu, Jvcai Li, and Peng Zhao. 2015. 'Estimating Crop Albedo in the Application of a Physical Model Based on the Law of Energy Conservation and Spectral Invariants', *Remote Sensing*, 7: 15536-60.

Philipona, Rolf, Andreas Kräuchi, and Emmanuel Brocard. 2012. 'Solar and thermal radiation profiles and radiative forcing measured through the atmosphere', *Geophysical Research Letters*, 39.

Román, Miguel O, Charles K Gatebe, Yanmin Shuai, Zhuosen Wang, Feng Gao, Jeffrey G Masek, Tao He, Shunlin Liang, and Crystal B Schaaf. 2013. 'Use of in situ and airborne multiangle data to assess MODIS-and Landsat-based estimates of directional reflectance and albedo', *IEEE Transactions on Geoscience and Remote Sensing*, 51: 1393-404.

Ross, Juhan. 2012. *The radiation regime and architecture of plant stands* (Springer Science & Business Media).

Roxy, MS, VB Sumithranand, and G Renuka. 2010. 'Variability of soil moisture and its relationship with surface albedo and soil thermal diffusivity at Astronomical Observatory, Thiruvananthapuram, south Kerala', *Journal of earth system science*, 119: 507-17.

Shantikumar, NS, S Jade, TS Shrungeshwara, and H-J Song. 2016. 'Validation of water vapor retrieval from Moderate Resolution Imaging Spectro-radiometer (MODIS) in near infrared channels using GPS data over IAO-Hanle, in the trans-Himalayan region'.

Shaw, RH. 1956. 'A comparison of solar radiation and net radiation', *Bull. Am. Meteorol. Soc*, 37: 205-06.

Shi, Jiancheng, Peng Guo, Tianjie Zhao, and Jinyang Du. 2014. "Soil Moisture downscaling algorithm for combining radar and radiometer observations for SMAP mission." In *General Assembly and Scientific Symposium (URSI GASS), 2014 XXXIth URSI*, 1-4. IEEE.

Shupe, Matthew D, and Janet M Intrieri. 2004. 'Cloud radiative forcing of the Arctic surface: The influence of cloud properties, surface albedo, and solar zenith angle', *Journal of Climate*, 17: 616-28.

Singh, Nilendu, Bimal K Bhattacharya, MK Nanda, Prafulla Soni, and Jai Singh Parihar. 2014. 'Radiation and energy balance dynamics over young chir pine (Pinus roxburghii) system in Doon of western Himalayas', *Journal of earth system science*, 123: 1451-65.

Sullivan, Patrick F. 1995. 'Mortality in anorexia nervosa', *The American journal of psychiatry*, 152: 1073.

Tian, Li, Yangjian Zhang, and Juntao Zhu. 2014. 'Decreased surface albedo driven by denser vegetation on the Tibetan Plateau', *Environmental Research Letters*, 9: 104001.

Wang, Kaicun, Jingmiao Liu, Xiuji Zhou, Michael Sparrow, Min Ma, Zhian Sun, and Wenhua Jiang. 2004. 'Validation of the MODIS global land surface albedo product using ground measurements in a semidesert region on the Tibetan Plateau', *Journal of Geophysical Research: Atmospheres*, 109.

Wang, Kaicun, Zhengming Wan, Pucai Wang, Michael Sparrow, Jingmiao Liu, Xiuji Zhou, and Shigenori Haginoya. 2005. 'Estimation of surface long wave radiation and broadband emissivity using

Moderate Resolution Imaging Spectroradiometer (MODIS) land surface temperature/emissivity products', *Journal of Geophysical Research: Atmospheres*, 110.
Webster, Clare, Nick Rutter, Franziska Zahner, and Tobias Jonas. 2016. 'Measurement of incoming radiation below forest canopies: A comparison of different radiometer configurations', *Journal of Hydrometeorology*, 17: 853-64.
Weligepolage, K, ASM Gieske, and Z Su. 2013. 'Effect of spatial resolution on estimating surface albedo: A case study in Speulderbos forest in The Netherlands', *International Journal of Applied Earth Observation and Geoinformation*, 23: 18-28.
Wilson, TB, and TP Meyers. 2007. 'Determining vegetation indices from solar and photosynthetically active radiation fluxes', *Agricultural and Forest Meteorology*, 144: 160-79.
Wizemann, Hans-Dieter, Joachim Ingwersen, Petra Högy, Kirsten Warrach-Sagi, Thilo Streck, and Volker Wulfmeyer. 2014. 'Three year observations of water vapor and energy fluxes over agricultural crops in two regional climates of Southwest Germany', *Meteorol. Z.*, 24: 39-59.
Wu, Xuejiao, Ninglian Wang, Anxin Lu, Jianchen Pu, Zhongming Guo, and Huawei Zhang. 2015. 'Variations in albedo on Dongkemadi Glacier in Tanggula Range on the Tibetan Plateau during 2002–2012 and its linkage with mass balance', *Arctic, Antarctic, and Alpine Research*, 47: 281-92.
Zhong, Qiang, and Li Yinhai. 1988. 'Satellite observation of surface albedo over the Qinghai-Xizang plateau region', *Advances in Atmospheric Sciences*, 5: 57-65.